Neuroradiology (1990) 32: 371–391

Neuro radiology

Cine MR in the evaluation of normal and abnormal CSF flow: intracranial and intraspinal studies

R. M. Quencer[1], M. J. Donovan Post[1], and R. S. Hinks[2]

[1] Department of Radiology, University of Miami School of Medicine, Miami, Florida, USA
[2] Picker International, Inc., Highland Heights, Ohio, USA

Summary. Evaluation of intracranial and intraspinal CSF flow was accomplished by the use of cardiac gated gradient echo magnetic resonance (MR) technique. Normal patterns of pulsatile flow within the ventricles, cisterns and cervical subarachnoid space were established by this technique and these observations were compared to prior description of CSF flow. With systole there is downward (caudal) flow of CSF in the aqueduct of Sylvius, the foramen of Magendie, the basal cisterns and the dorsal and ventral subarachnoid spaces while during diastole, upward (cranial) flow of CSF in these same structures is seen. The relationships between the cardiac cycle and the CSF pulsations are demonstrated on both magnitude reconstruction and phase reconstruction MR images. Calculations of actual fluid velocity within CSF containing spaces can be obtained from the phase reconstruction images and holds promise for a more accurate analysis of CSF flow. In conditions which result in alterations of flow, cine MR dramatically shows either obstruction or excessively turbulent flow within the CSF pathways. The site of obstructed flow whether in the third ventricle, aqueduct, fourth ventricle, or subarachnoid space can be appreciated by changes in or absence of the normal hypointense signal. Cystic cord lesions such as congenital syringohydromyelia and posttraumatic spinal cord cysts may show pulsatile flow of CSF, a fact which can relate to progressive enlargement of these cysts. The distinction between myelomalacia and cyst formation in the cord is facilitated by the technique. Although the use of cine MR for the analysis of CSF flow is in its infancy, our experience indicates that this technique is useful in a wide range of pathological conditions including, but not limited to, conditions resulting in hydrocephalus or cystic cord lesions.

Key words: Magnetic resonance imaging – Cerebrospinal fluid flow – Hydrocephalus – Spinal cord cyst – Cine-MR

Over the years, the nature and significance of pulsatile intracranial and intraspinal CSF flow has been the object of a number of investigations and much conjecture. In an attempt to clarify many of these issues, Du Boulay in 1966 and 1972 [1, 2] reported the use of radiological techniques to measure pulsations of CSF during pneumoencephalography, myelography and ventriculography. He made a number of important observations, including the fact that pulsations in the normal cervical subarachnoid space paralleled arterial pulsations, and that these CSF pulsations diminished below the upper thoracic region. He was led to conclude that CSF pulsations at the aqueduct arise from a pumping mechanism of the thalamus, that flow in the basal cisterns is a consequence of the rhythmic expansion and contraction of the brain during systole and diastole, that previously held theories concerning the choroid plexus and the source of CSF pulsations were incorrect, and that causes of CSF movement are ultimately related to the pressure and elasticity provided by the arteries and veins.

Lane and Kricheff in 1972 [3] published their observations on normal and abnormal cervical CSF pulsations using a videodensitor display of Pantopaque myelography. Their measurements were taken directly off a television monitor and showed a wide range of deflection (3–30 mm) in the upper cervical spine. Importantly, they demonstrated, in normal patients, caudal pulsations in systole and cranial pulsations in diastole while in patients with obstruction of the spinal CSF pathways, they demonstrated a lower pulsation amplitude above and below the block. The unavoidable problem involved in these early studies was the fact that measurement and evaluation of CSF flow involved the injection of contrast material into the CSF spaces and/or the evaluation of the movements of "foreign" material (e.g. oil-based contrast material) in the CSF spaces. Although such methods provided some information concerning CSF dynamics they were, by their very nature, invasive and therefore disturbed the very system they were meant to investigate. Furthermore, these investigations could not provide simultaneous characterization of flow dynamics in multiple areas of the subarachnoid space, nor could they easily calculate CSF velocity.

With magnetic resonance imaging (MR) however, the ability to evaluate CSF flow has improved. In general, the MR signal obtained from a body part depends on a num-

ber of factors. For stationary tissues these include proton density, T1 and T2, along with the pulse sequence parameters (TR, TE, flip angle) which are chosen. When however, there is fluid movement such as is seen with flowing blood or CSF, the signal obtained from that area depends on a number of additional factors, including direction of fluid flow, field and gradient strengths, slice thickness and position, the presence or absence of motion compensating gradients, and the velocity and type of motion the fluid experiences. These factors have an effect on phase shifts and on variations in signal intensity from view to view, thus causing the well recognized flow voids. Because of this and because no invasive procedure is perforemd and no contrast material is introduced, MR imaging is a nearly ideal modality for the assessment of CSF flow.

A number of MR observations and techniques have been employed to take advantage of signal changes attendant to CSF flow. The CSF flow void sign was described a number of years ago by Sherman and Citrin [4] and this phenomenon was shown to be related to the cardiac cycle [5]. Similar observations concerning CSF flow voids in the spinal canal were reported by Sherman [6]. Although with routine spin echo or gradient echo MR in which no flow compensation techniques are used one may frequently appreciate the effect of CSF flow, the visualization of these flow voids is not consistent and the degree to which such flow is abnormal may not be obvious. When the CSF flow void is absent in areas where it is normally expected (e.g. aqueduct), inferences can be made concerning the obstruction along these CSF pathways [7]. Furthermore, Bradley [8] described an abnormally pronounced aqueductal flow void phenomena in patients who presented with normal pressure hydrocephalus and related this to ventricular compliance and surface area. Later he described a relationship between this flow void and deep white matter infarcts [9]. Rubin [10] described a technique in which gradient echo images were obtained using two or three different flip angles and the amplitude of the CSF pulsations were calculated and related to interval flow (or volume) of CSF. Atlas [11] used an axial single slice gradient echo technique to evaluate aqueductal patency and found that in normals, a bright signal was seen within the aqueduct, whereas a dark signal was present when there was aqueductal obstruction. This is similar to what has been used to distinguish flowing blood from vascular obstruction. A technique described by Njemanze and Beck [12] which evaluated CSF pulsatile flow, utilized two gradient pulses of equal magnitude but opposite sign and these were applied during a long TR sequence. With this non-cine MR subtraction technique, moving protons are not brought back into phase, resulting in a phase shift which relates to fluid flow. When cardiac gating is used, such images can be obtained both in systole and diastole and flow variations in CSF containing spaces can be visualized.

We have studied CSF flow dynamics in a different manner by employing a technique of cardiac gated, gradient echo MR imaging in which the acquired data is displayed as magnitude and/or phase reconstructed images in a closed loop cine format. From such images and data both qualitative and quantitative assessments of CSF flow can be made [13–17]. The qualitative cine MR allows a rapid and dramatic evaluation of both normal and abnormal patients in a visual form pleasing to both the radiologist and the referring clinician. Quantitative evaluation of CSF flow via phase reconstruction permits a more precise mapping of the intracranial and intraspinal flow patterns, is more sensitive in detecting fluid motion and allows calculation of CSF velocity. We herein present our observations with this cine MR technique and report what we believe to be its clinical value.

Technique and theory

Using a 1.5 T (Picker[1]) superconducting magnet, head and spine cine images were obtained in the mid-sagittal plane. Occasionally, axial and/or coronal images were obtained but in the vast majority of patients, mid-sagittal scans were preferred because this is the plane of examination which displays CSF pathways in continuity. Limited studies thus far have been done in the lumber region so the majority of our observations concerning intraspinal flow relate to the cervical and thoracic regions. We emphasize that this investigation analyzes the pulsatile motion of CSF, not the slow bulk flow of CSF.

All the CSF flow studies are cardiac gated and use a reduced flip angle (10 degrees) gradient echo technique with a TR determined by the patient's R-to-R interval, a TE of 18 ms, and a section thickness of 6 mm. Multiple images ("cine frames") in the same plane are obtained during an R-to-R interval, starting immediately after the R-wave and acquiring successive images at 50 ms intervals to within about 200 ms of the next R-wave. For example, if there are 60 beats per minute (or 1 beat every 1000 ms), the number of images which would be available for cine viewing would be 16 (1000 ms – 200 ms dead time)/50 ms, where 50 ms represents the relative spacing of the successive images (or, "cine frame rate"). The 200 ms dead time is used to allow the scanner to wait for the next heartbeat, thus improving the timing and accuracy of the cine study. Clearly, with a slower heart rate, more frames would be obtainable. The information is then displayed in a 'real time' closed loop cine format. Patients with cardiac arrhythmias are not ideal candidates for the gated studies because of the varying R-to-R interval.

Images are acquired following 2 to 4 excitations, on a 128 or 192×256 matrix and displayed on a 512×512 matrix. Two dimensional Fourier transformation is employed. Intracranially, our early work utilized a linear drive head resonator, but recently we have used a quadrature head coil (transmit and receive). Intraspinal evaluations have employed a rectangular surface coil (receive only). The spine studies are all done with the neck in a neutral position because of the potential of changing the CSF dynamics as a consequence of varying the neck positions. In nearly all cases, the cine examination was performed following the completion of a routine brain or spine study. It added approximately 15 min to the total

[1] Picker International, Inc., 5500 Avion Park Drive, Highland Heights, Ohio 44143, USA

examination time. Occasionally when time did not permit, the patient had to be rescheduled for a cine study on another day.

The ability of this MR cine flow technique to visualize flowing CSF is dependent upon proper timing and strength of the spatial gradients. Specifically, the dipolar gradients can be modified in terms of duration, amplitude, and separation between pulses in such a manner as to accentuate the dephasing effect of moving protons as they pass through the gradients. These modified gradient pulses are most commonly applied in the plane of the acquired images. The theory of application of these gradients is exactly opposite to the use of gradients to suppress fluid motion as has been reported with various forms of gradient moment nulling [18–20]. The result of these gradient profile manipulations is to produce a cine study in which a marked signal loss of flowing CSF stands out in contrast to stationary or slow flowing CSF. Because we most frequently evaluate sagittal cine studies, the extra gradient pulses are applied along the frequency (i.e. the vertical) encoded axis, causing flow sensitization along the cranial-caudal axis.

Quantitative flow (or what may be referred to as flow maps or phase maps) are computed from sets of flow sensitized and flow desensitized images. In essence, (a) flow sensitized studies contain phase shifts due to flow, magnetic field inhomogenity, magnetic susceptibility, and chemical shift, while (b) flow desensitized studies contain no phase shifts due to flow but retain phase shifts due to these other factors. These sequences (a and b) which are acquired at the same time in an interleaved fashion, are subtracted from each other resulting in data which reflects phase shifts due to flow. Since correlations between phase shifts and flow have already been established by calculations ($\varnothing = \int G(t)vtdt$, where $\varnothing$ is the phase shift, G is the gradient strength applied, v is the velocity of the flowing material, and t is the elapsed time) and by phantom models [15], a scaled relationship between phase shifts (0–360 degrees) as seen on the flow maps and CSF velocity can be calculated. The result is that the gray scale intensity of each pixel is directly related to the velocity of CSF (mm/s) at that point. These flow maps can also be displayed in a cine mode so that two sets of images are available for interpretation – one a magnitude (qualitative) cine study, the other a phase (quantitative) or flow map. Because it reflects phase shifts, the flow map is far more sensitive to CSF flow than is the magnitude cine study and can be used to determine the rate and direction of CSF flow at any point during the cardiac cycle. As a convention caudal flow of CSF is seen as a hyperintense signal on the phase maps, whereas cranial flow of CSF is seen as a hypointense signal.

We have recently employed a second method of quantitating CSF flow (not demonstrated in this paper) which employs an axial presaturation pulse. The effect of this pulse is to turn a given volume of CSF hypointense. The movement of this "slab" or bolus of presaturated CSF can be followed caudally throughout the cardiac cycle and by measuring the distance the slab moves (bolus tracking) and knowing the cine frame rate, the velocity of CSF can be calculated (in mm/s).

Subjects

During the past two years, we have studied over 200 patients with intracranial and intraspinal cine MR examinations. Our subject material comes from (a) normal volunteers, (b) patients not clinically suspected nor subsequently demonstrated to have CSF flow abnormalities and (c) patients with clinically suspected and/or subsequently proven CSF flow abnormalities. In the majority of cases, only a qualitative cine study was performed, however ample numbers of patients have been studied with the quantitative technique to allow preliminary estimations of normal CSF flow velocities and determination of the direction of flow. Normal blood pressure and pulse pressure was present in all our normal volunteers and it was likewise normal in all those patients whose blood pressure was taken at the time of the examination. In those patients whose blood pressure was not taken at the time of study, a review of the available records showed no evidence of hypertension.

There was a wide variety of clinical situations in which a CSF cine examination was performed. In the spine, this included: evaluation of cord cysts (posttraumatic, congenital) for degree and extent of cyst pulsatility; distinguishing cystic myelomalacia (posttraumatic) from cord cysts; evaluation of arachnoid/subarachnoid cysts (congenital, postoperative, or posttraumatic) for their extent and pulsatility; determining the degree of block of CSF flow within the thecal sac. Intracranially, the majority of examinations were performed in patients with hydrocephalus in an attempt to distinguish between the various causes of ventriculomegaly (atrophy, aqueductal stenosis or insufficiency, normal pressure hydrocephalus) or to determine the effect of intracerebral masses on CSF dynamics. Occasionally, patients were studied with cine MR who had no hydrocephalus but who nonetheless could have had disturbances in CSF flow, such as: pseudotumor cerebri, Chiari I malformation; intracranial mass; postoperative shunting or craniotomy; or posttraumatic changes.

Observations and comparison with previous investigations

The qualitative cine studies were examined for evidence of marked signal void within various CSF pathways indicative of pulsating and rapidly flowing CSF. Intracranially, we examined primarily the aqueduct of Sylvius, the third ventricle, fourth ventricle, foramen of Magendie, dorsal and ventral subarachnoid spaces at the cervico-medullary junction, and the pre-pontine and pre-medullary cisterns. Within the spine we assessed flow in the dorsal and ventral subarachnoid spaces. The CSF pathways were judged to be patent whenever a normal flow void was observed during a portion of the gated cycle. Flow patterns within abnormal CSF containing structures (e.g. cysts or obstructed CSF pathways) were also evaluated. When quantitative flow studies (phase maps) were done, they were compared to the qualitative cine studies in order to see which gave a

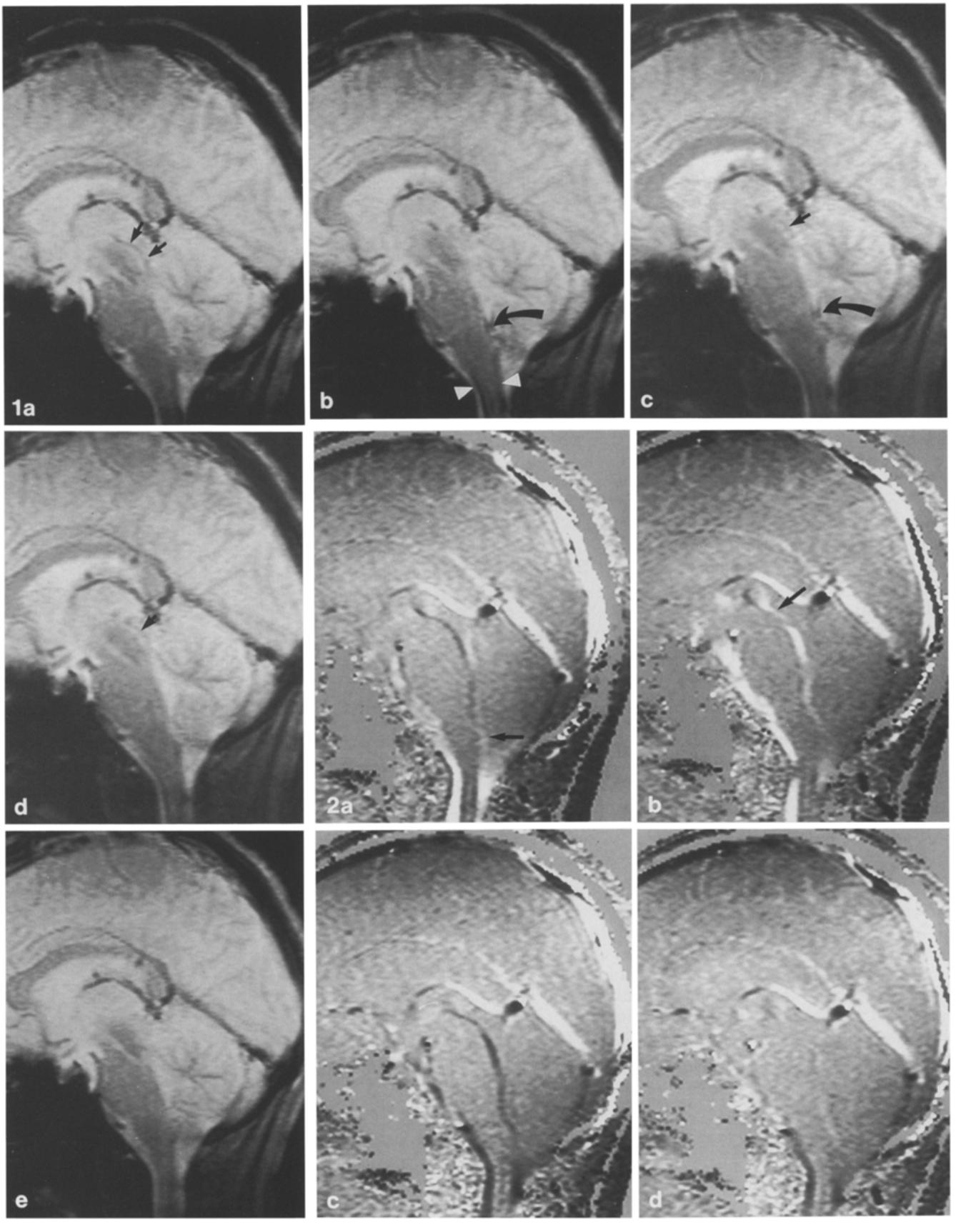
1a
b
c
d
2a
b
e
c
d

more sensitive indication to the presence of CSF flow. In a few cases, actual CSF flow velocities were determined.

Normal intracranial CSF flow (Figs. 1, 2)

Qualitative assessment (Fig. 1)

In normals, a flow void in the aqueduct is always seen. This pulsatile downward wave of CSF movement is maximally displayed 175 to 200 ms following the R wave, however it is usually preceeded by CSF flow out of the fourth ventricle through the foramen of Magendie. Pulse wave propagation is seen along the entire length of the aqueduct, however a hypointense flow void is not seen throughout the fourth ventricle; rather the flow void can be seen in the very rostral portion of the fourth ventricle where it is continuous with the aqueduct and in the caudal fourth ventricle where it is continuous with the foramen of Magendie. Midway through the cycle, a cephalad wave of CSF can be seen pulsing retrograde through the aqueduct, when combined with the caudal component of flow, a movement which is best described as a 'to-and-fro' motion of CSF. After the retrograde pulse of CSF, a period of fluid quiessence is noted where no fluid motion is detected. Variable degrees of CSF flow within the posterior third ventricle are observed and occasionally flow at the level of the foramen of Monro is seen. The reason for the sporadic visualization of the foramen of Monro is explained by the fact that the structure may be out of the plane or may be volume averaged with aqueduct material by our standard 6 mm thick mid-sagittal sections.

As a result of volume changes of the brain during the cardiac cycle, flow of CSF in the basal cisterns is expected. As opposed to the relative constancy of hypointense signal in the aqueduct and foramen of Magendie, the flow into the basal cisterns is far less noticeable on the magnitude images (Fig. 1). In fact, a surprising qualitative difference in CSF flow was noted above and below the foramen Magnum, a finding in keeping with one of Du Boulay's original observations [1]. Specifically, higher flow is seen just below the foramen magnum when compared to the less rapidly flowing CSF above the foramen magnum. This disparity is undoubtedly related to the size of the CSF spaces anterior to the brainstem. CSF flow maps (Fig. 2) which are more sensitive to fluid motion, clearly demonstrate CSF flow in these cisternal areas. In comparison with the areas of obvious CSF flow voids described above, similar pulsatile or turbulent flow was not noted within normal lateral ventricles except in the area directly adjacent to the foramen of Monro. This observation is explained by the fact that CSF flowing through large areas within the lateral ventricular system does so with a lessened fluid velocity and negligible turbulence.

Quantitative assessment (Fig. 2)

On the flow maps (phase images), one can more easily identify both the antegrade (caudally directed) and retrograde (cephalad directed) CSF movement. Such motion reflects an expansion of the brain during systole, forcing the CSF downwards and then a relaxation of the brain during diastole, during which CSF flows superiorly. In both intracranial and intraspinal studies, varying CSF velocities throughout systole and diastole can be calculated. Assessment of CSF dynamics with flow maps is, in our opinion a more accurate and more easily interpreted representation of fluid flow than the qualitative cine MR (compare Fig. 1 with Fig. 2).

Because of the small size of the aqueduct of Sylvius (normal 2–3 mm) relative to the slice thickness of the sagittal image (6 mm), it is difficult to obtain an accurate calculation of CSF velocity through this structure. Since the flow determinations are based on changes in signal phase within a voxel, volume averaging will cause static material to be average into those voxels which encompass the aqueduct. This can result in a calculated CSF velocity less than the true velocity. With these limitations in mind, aqueduct flows in the caudal direction were measured in six normal volunteers and the velocities ranged from 3.7 to 7.6 mm/s. Axial cine examinations through the aqueduct yield more accurate velocity information because measurements through the plane of the flow could be made. For this to happen, pixel size should be onethird the size of the aqueduct so that at least one pixel in a given slice would have no volume averaging with surrounding static material. For an aqueduct of 3 mm, a 1 mm × 1 mm in-plane resolution would be required, a capability which we have chosen not to utilize because of the diminished signal-to-noise which would result given the scanning time used. Recent

Fig. 1a–e. Normal intracranial CSF flow. Mid-sagittal cine CSF flow study with qualitative (magnitude) reconstruction is seen here as five frames out of a total of twelve. Flow in the aqueduct (*arrows* in **a**) commences after the R wave. Midway through the cycle, a cephalad wave of CSF could be seen on the cine loop pulsing retrograde through the aqueduct (*arrows* in **c** and **d**), a movement best described as a "to-and-fro" motion of CSF. Visualization of a flow void through the foramen of Magendie (*curved arrows* in **b** and **c**) is expected in normals, however differences in size and degree of signal hypointensity between patients is expected. This relates to the variable size of the foramen of Magendie and its course relative to the mid-sagittal plane. After the retrograde pulse of CSF, a period of relative fluid quiessence is seen where little fluid motion is detected **(e).** Flow in the ventral and dorsal subarachnoid space at C1 and C2 is outlined by *white arrowheads* in **b** and can be seen in other frames also. Phase mapping (Fig. 2) can more dramatically depict fluid motion in areas of slower fluid flow. CSF flow both intraspinally and intracranially, while seen adequately on a static display such as this, is seen more dramatically on a closed loop cine display

Fig. 2a–d. Normal intracranial CSF flow (flow map). In these four frames from a cine flow map (not the same patient as Fig. 1), caudal flow of CSF is hyperintense, cranial flow is hypointense. Caudal CSF flow in the basal cisterns and spinal CSF spaces and faint flow out of the foramen of Magendie (*arrow* in **a**) appears to preceed the downward pulsation of CSF through the aqueduct. In fact, there is still some cephalad flow in the aqueduct in this early frame **(a).** Caudal flow in the aqueduct then follows (*arrow* in **b**) later in the cardiac cycle. In diastole with decrease in brain volume, cranial flow (areas of hypointense signal) of CSF in the cisterns and ventricular system is noted **(c).** In **d,** note the relative quiessence of CSF flow prior to the next R wave (analogous to Fig. 1 e). From such flow maps velocities can be calculated (see text). When this figure is compared to Fig. 1, the increased sensitivity of such a sequence to flow is obvious. Note, for example, the obvious flow in the pre-pontine and pre-medullary cisterns

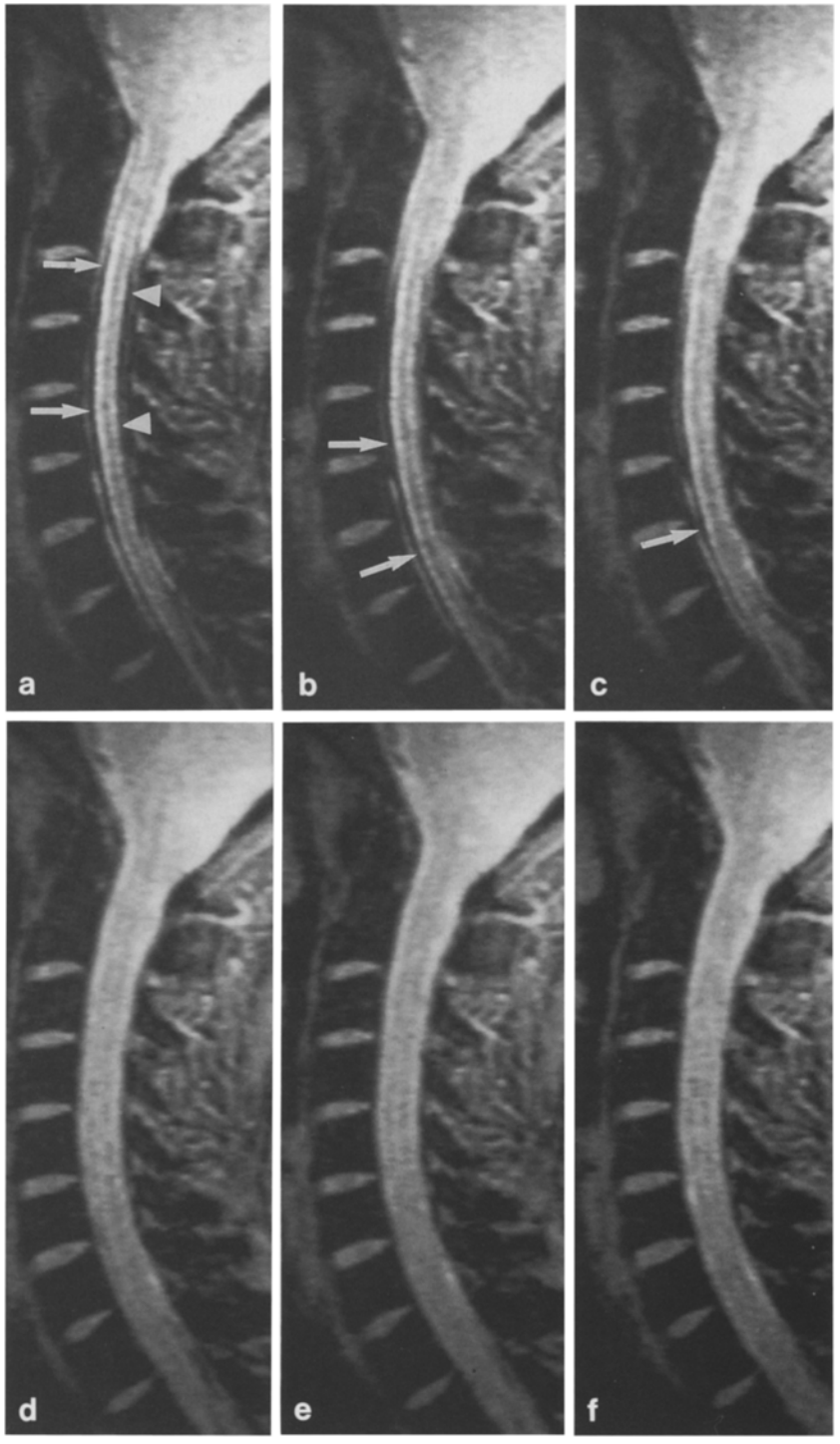

Fig. 3 a–f. Normal intraspinal CSF flow. Midsagittal CSF study with qualitative (magnitude) cine MR shows 6 out of a series of 12 images. Flow (signal hypointensity) in the ventral SAS (*arrows* in **a–c**) is more prominent than in the dorsal SAS (*arrowheads* in **a**). Flow of the CSF diminishes later in the cardiac cycle **(d–f)** so it appears that there is no flow of CSF in either a cranial or caudad direction. Phase imaging (see Fig. 4) shows however, that there is a constant bidirectional movement of CSF within the spinal canal

reports of axial cine imaging have been presented [21, 22], however the spatial resolution of the technique used has not been published. Despite the fact that it is difficult to precisely measure flow velocity in the aqueduct, the flow maps do dramatically display the CSF flow dynamics.

In the fourth ventricle and foramen of Magendie, flow caudal and cephalad flow are clearly depicted. Interestingly, we observed that flow out of the inferior portion of the fourth ventricle into the foramen of Magendie is not simply a continuation of the flow from the aqueduct. Such asynchrony may result from pulsations of the choroid plexus of the fourth ventricle and/or expansion/contraction of the stem itself which does not occur at the same time as thalamic expansion/contraction. In fact, the caudally directed CSF pulse wave is observed to start first in the fourth ventricle, followed later (by 100–150 ms) by caudal flow in the aqueduct. Cranial flow of CSF back through the aqueduct may still be occurring when the first downward pulsation through the foramen of Magendie is seen (see Fig. 2). Clearly therefore, this cephalad aqueductal CSF flow is not simply the result of retro-

grade flow from the basal cisterns into the fourth ventricle and upwards. Non-synchronous flow can be observed occurring in both directions, and can be noticed in many segments of the CSF pathway. As stated above, the probable reasons for these normal variations are multiple but relate most likely to the size of nearby vasculature, the compliance of surrounding brain/spinal cord tissue, the anatomy of the CSF containing spaces, the volume and vascularity of the choroid plexus, and the systemic hemodynamics.

Normal variations in the size of the foramen of Magendie cause difficulty in accurate *measurement* of CSF flow (although such flow is always *visualized* more readily on the flow maps than on the qualitative [magnitude] images). The same limitations of size as described above under the aqueduct pertains here. In five of six normal volunteers in whom flow in this area was measured, the values ranged from 2.4–5.6 mm/s. The sixth volunteer had a value of 12.5 mm/s. At this time, we have only a small number of patients in whom quantitative measurements of intracranial and intraspinal CSF flow have been made. Our preliminary experience indicates however, that large variations in normal velocities should be expected in all CSF spaces.

Velocity measurements in the basal cisterns and upper cervical subarachnoid space are felt to be more reliable than those velocity measurements obtained from smaller spaces such as the aqueduct of Sylvius. The phase imaging (Fig. 2) clearly demonstrates a caudally directed flow followed by a cranial flow in both the upper cervical spine and in the pre-medullary and pre-pontine cisterns. We have performed some preliminary measurements on the caudal flow component. Peak caudal velocity ranges of 7.8 to 38.1 mm per second in cisterns anterior to the brain stem have been observed. The reason for the wide range of these values relates primarily to the anatomical size of the structure through which the CSF must pass and this of course, varies from patient to patient. If for example, the pre-medullary cistern is relatively small, the CSF velocity would be higher for a given volume of fluid than if the space were capacious. The distensibility of the venous structures must also play a role in the pulse wave effects as Du Boulay has pointed out [1, 2].

Normal intraspinal CSF flow (Figs. 3, 4)

Qualitative assessment (Fig. 3)

In normal patients, flow in the ventral and dorsal cervical subarachnoid space is observed. It is common to observe more prominent ventral CSF flow because the ventral SAS is wider. Close inspection of these images show a variation in intensity of the signal voids across a given plane. This reflects the fact that near the dura or cord there is a wider range of phase shifts (i.e. dephasing) than there is in the center of the SAS.

Quantitative assessment (Fig. 4)

As in the brain, the flow maps of the spine (Fig. 4) are more sensitive to CSF flow (hyperintense-caudal; hypointense-superior flow) than the qualitative examinations (compare Fig. 1 to 2 and Fig. 3 to 4). Velocity calculations show a greater flow velocity in the inferior direction compared to the superior direction. We have found normal peak CSF velocities in the anterior cervical SAS at C2 to range from 10.9 to 52.4 mm/s. Itabashi [23] reported peak CSF velocities in the cervical spine of 50–100 mm/s which increased when the neck was flexed and the change in direction of CSF flow occurred earlier with neck flexion. Differential flow at various spinal levels exists as the flow propagates inferiorly through narrow and then wider spaces. At disc space levels and wherever pathological narrowing (short of complete obstruction) occurs, CSF velocities would be expected to increase. Enzmann [22] found that in his normal population the highest CSF velocity in the cervical spine was at the C6 level because the canal area was smallest there.

Typically, caudal flow within the cervical subarachnoid space commences approximately 100–150 ms following the R wave and maximum velocity is, on the average, reached 75–100 ms later (i.e. 175–250 ms after the R wave) [14]. Thereafter, the flow decreases and then reverses so that cranial flow of CSF occurs later in the cardiac cycle (400–500 ms after the R wave). We have studied a number of thoracic and lumbar spines with this technique and have observed that maximum flow occurs later (300–400 ms after the R wave in the lumbar spine) in those areas other than in the cervical area and the velocity of CSF flow is lower (17–28 mm/s in the lumbar spine) in these regions. This finding is similar to the observations made by Du Boulay [1] with oil contrast in which he noted diminished pulsations below the upper thoracic cord level. The relationship between aqueductal flow and flow in the cervical SAS was explored by Enzmann [22] and he found that aqueductal flow occurred later in the cardiac cycle than cervical CSF flow. No explanation for this apparent lag was offered, however asynchrony in arterial pumping at the thalamic versus the lower brain stem level could explain this tendency and appears in concert with our observations (described above) that pulsations out of the fourth ventricle via the foramen of Magendie appears to occur *prior* to the pulse wave through the aqueduct.

Estimates of cord motion by other investigators have been made on phase images similar to images seen in Fig. 4. Levy [24] suggested that when the signal of the cord became brighter, a caudal movement of the cord was occurring and he calculated that movement to be approximately 12.6 mm/s in normals. With his images a complex relationship between this downward movement of the cord and the CSF flow appeared to exist. At certain points during the cardiac cycle, the cord appeared bright (caudal cord movement) but the CSF was dark (cranial CSF flow). We have not investigated cord motion and its relationship to CSF flow.

In summary, the information and observations obtained from the analysis of normal intracranial and intraspinal CSF flow indicates that pulsatile flow occurs as a consequence primarily of the expansion of the brain during systole. Flow occurs in both caudal and cranial directions. Intracranially, the caudal flow of CSF commences

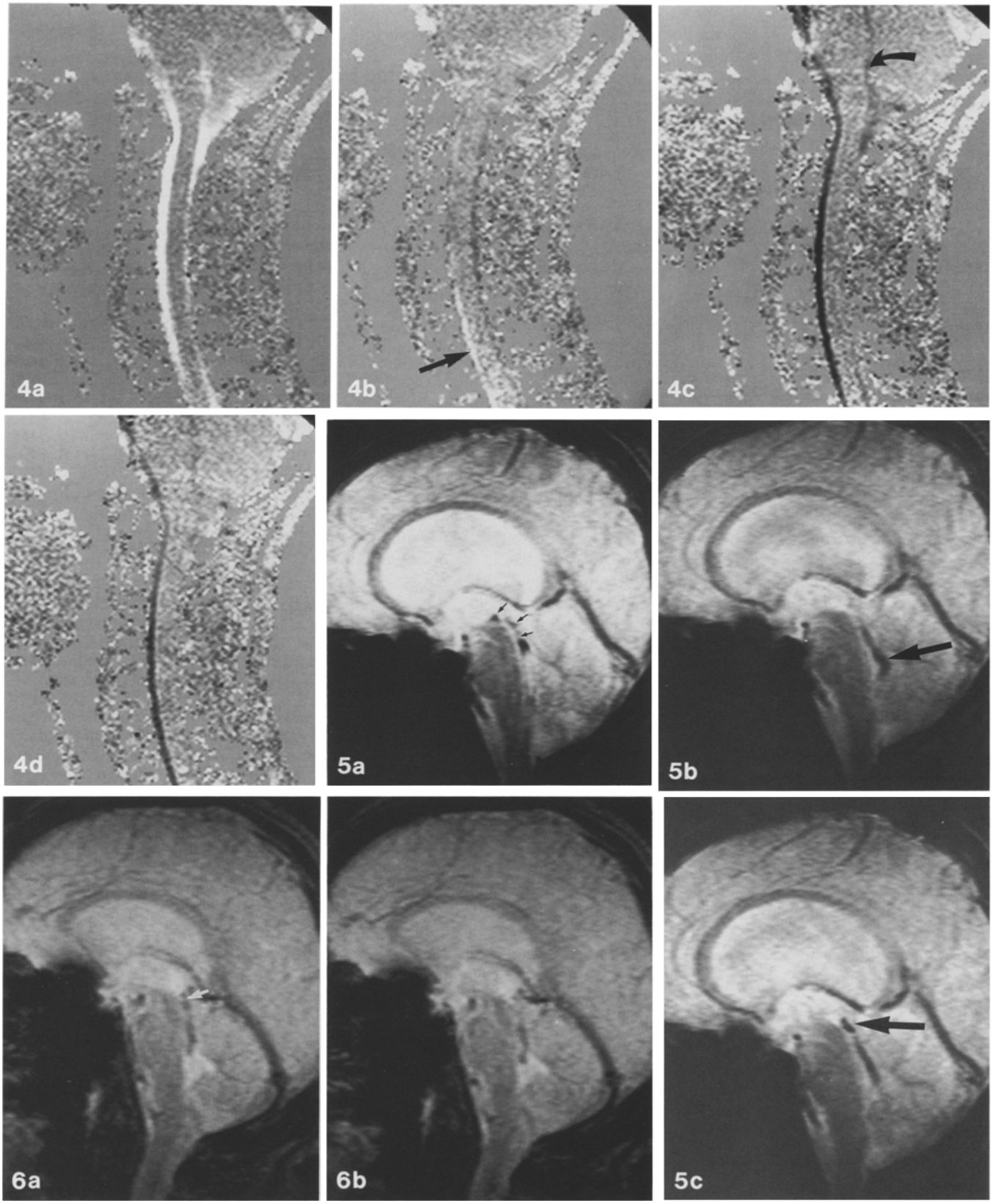

Fig. 4a–d. Normal intracranial spinal CSF flow. Mid-sagittal CSF study (not the same patient as Fig. 3) shows 4 out of a series of 12 frames of a cine MR (phase images). The anatomical landmarks are more difficult to discern compared to Fig. 3, but nonetheless show the caudal flow of CSF in systole (hyperintense indicates caudal flow) in **a.** Note the dramatic display of CSF flow in the anterior cisterns at the cervico-medullary junction and in the foramen of Magendie and cisterna magna region. In **b,** the flow of CSF in the ventral SAS in the mid to lower cervical region is noted (*arrow* in **b**). By the third frame **(c)** cranial flow of CSF is seen (displayed as hypointense signal) and this superior flow is more pronounced in the ventral SAS. Note also cephalad flow of CSF from the cisterna magna into the foramen of Magendie (*curved arrows* in **c**)

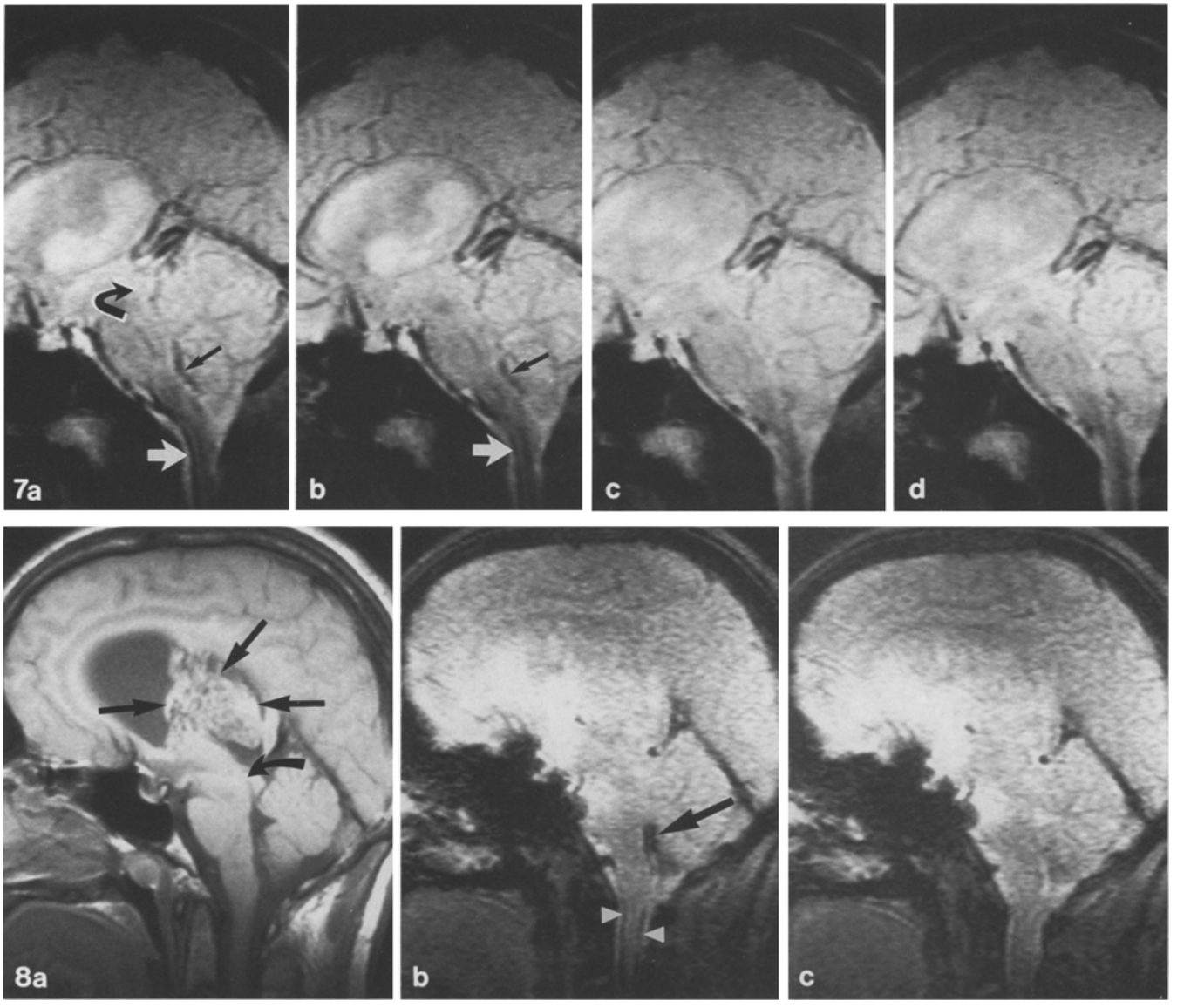

Fig. 5 a–c. Turbulent flow in fourth ventricle in patient with cerebral atrophy. Routine axial MR demonstrated hydrocephalus (not shown) in a patient with none of the clinical criteria for NPH. Cine MR (3 out of 12 frames) shows turbulent flow of CSF within the fourth ventricle (*arrow* in **b**) following a normal pulse wave of CSF through the aqueduct (*arrows* in **a**). In **c,** retrograde (or cranial) CSF flow back through the aqueduct (*arrow* in **c**) is seen (a finding far more striking on the closed loop cine display). The turbulent pattern here is nearly identical to that seen in one of our patients with classic NPH. The patent aqueduct rules out complete aqueductal occlusion as a potential cause of hydrocephalus. The direction of CSF flow cannot easily be determined from these static images. Phase images assist in that regard (e. g. see Fig. 2)

Fig. 6 a, b. Normal CSF flow pattern in a patient with a strong clinical history of NPH. In this patient with the typical triad of NPH (dementia, urinary incontinence, gait apraxia), normal pressure on lumbar puncture, and ventriculomegaly, the flow pattern (**a** and **b**) is nearly the same as that seen in normals (compare to Fig. 1). These two midsagittal frames show a patent aqueduct (*arrow* in **a**) and continuation of the flow void pattern into the rostral fourth and mid-fourth ventricular level. A hyperdynamic state of CSF flow is not seen. Radionuclide cisternography showed abnormal penetration into the ventricular system at 6, 24 and 48 h. Despite the relatively normal flow pattern on cine MR, the other signs for NPH were so strong that a ventricular peritoneal shunt procedure was performed. The patient showed a markedly improved clinical picture and continues to do well 6 months following the CSF diversionary procedure. Another patient with NPH had a flow pattern similar to Fig. 5, indicating a variability in CSF flow abnormalities in that disease

Fig. 7 a–d. Absent aqueductal flow void; aqueductal stenosis. Hydrocephalus without atrophy was noted on T1WI. Four frames from a cine MR demonstrate marked ventriculomegaly and lack of CSF flow through the aqueduct (*bent arrow* in **a** points to where normal flow void in aqueduct would be expected at this point of cardiac cycle). Despite this, CSF flow out of the 4th ventricle, through the foramen of Magendie and into the cisterna magna (*black arrows* in **a** and **b**) is seen. Note also CSF flow in the ventral SAS at the cervicomedullary junction (*white arrows* in **a** and **b**). Later in the sequence (**c** and **d**), flow through the fourth ventricular outlet diminishes and hypointensity at the level of the foramen of Magendie is no longer seen

Fig. 8 a–c. Absent aqueductal flow void; aqueductal compression. A large intraventricular ependymoma (*arrows* in **a**) has caused secondary compression of the midbrain, distortion of the tectum and narrowing of the rostral aqueduct (*curved arrow* in **a**). Flow through the aqueduct is absent (**b** and **c**); nonetheless CSF flow from the fourth ventricle into the cisterna magna is present (*arrow* in **b**). Note in **b** fluid flow in the ventral and dorsal SAS *(arrowheads)*

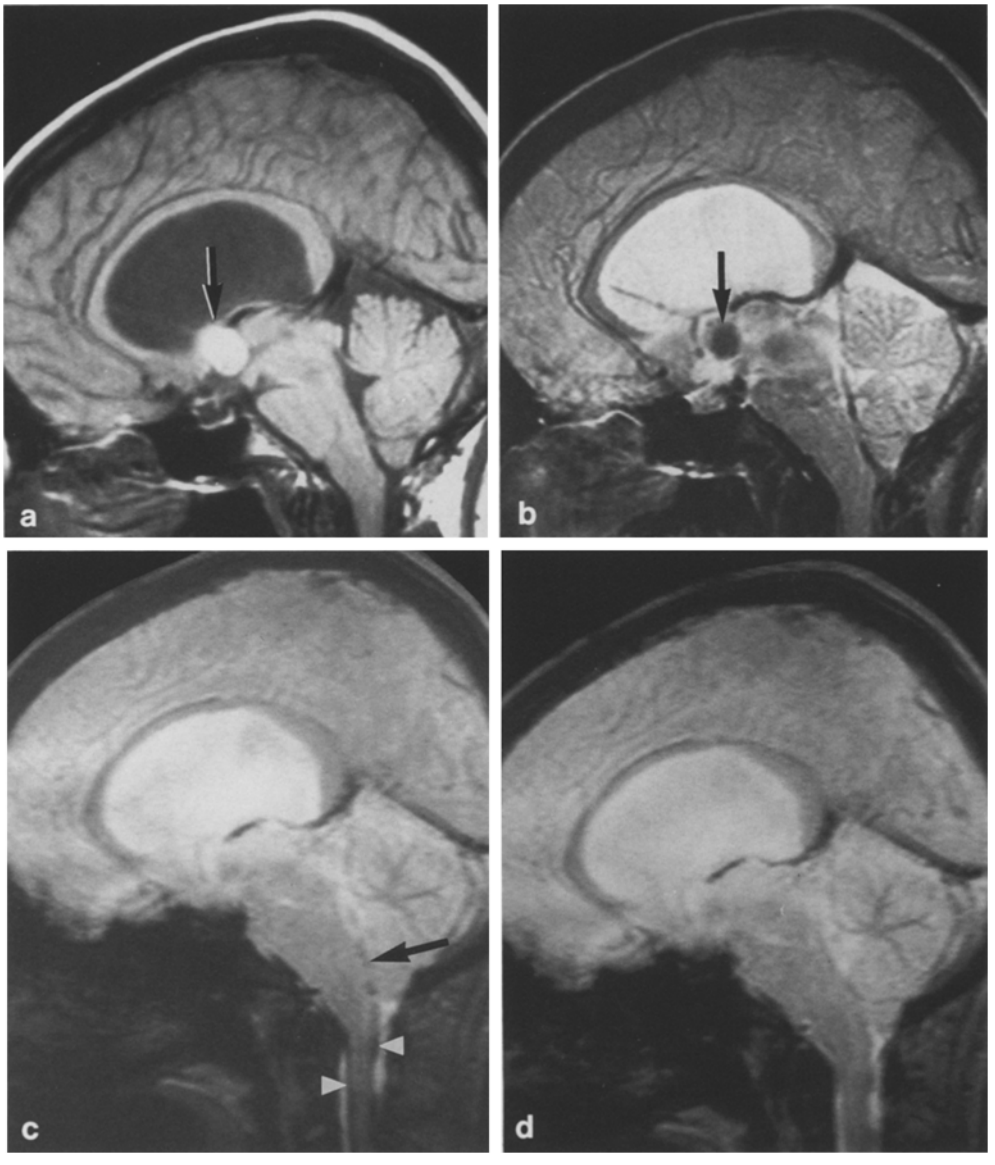

Fig. 9a–d. Absent aqueductal flow; third ventricular mass. On T1- **(a)** and T2- **(b)** weighted sagittal images, a colloid cyst of the third ventricle (*arrows* in **a** and **b**) has resulted in hydrocephalus because of obstruction at the level of both foramina of Monro. Normal CSF flow from the third ventricle through the aqueduct into the fourth ventricle is not present. Note the lack of flow void through the aqueduct on cine MR (**b** and **c** are 2 frames out of a total of 14 images). Nonetheless, there is flow out of the fourth ventricle (*arrow* in **c**) and flow in the ventral and dorsal SAS (*arrowheads* in **c**)

soon after the peak of the R wave and is first identified in the outlet of the fourth ventricle at the level of the foramen of Magendie. Within milliseconds thereafter, flow through the aqueduct is seen. It appears therefore that CSF flow does *not* occur as a continuum from the posterior third ventricle to aqueduct to fourth ventricle to foramen of Magendie but rather pulse waves may be generated independently in different parts of the CSF pathways, giving rise to what could be termed an "asynchronous propagation" of CSF flow. Similarly, asynchronous cranial or retrograde flow can be observed as venous drainage and hence, cerebral relaxation occurs. The downward flow of CSF within the spinal canal is greatest in the cervical region and is most noticeable in the ventral SAS. Expansion of the brain during systole with flow caudally from the basal cisterns and ventricular system generates this caudal CSF flow. Subsequent cranial flow in the SAS during diastole is observed. It is emphasized that this cine analysis reflects pulsatile CSF flow, not the bulk flow of CSF.

Alterations of intracranial CSF flow

Hyperdynamic flow

In patients with hydrocephalus, the CSF flow patterns vary according to the underlying cause for the enlarged ventricles. We have observed "hyperdynamic flow" in the fourth ventricle in a number of patients and this pattern (Fig. 5) clearly differed from flow of CSF in normal subjects (Fig. 1). We have examined only two patients who fulfilled the strict clinical criteria for NPH; one patient demonstrated markedly hyperdynamic fourth ventricular flow (similar to that seen in Fig. 5) but to date, that patient had not been shunted, while the other patient with NPH, surprisingly had what we judged to be a relatively normal flow pattern (Fig. 6).

Lack of aqueductal flow

Failure to demonstrate flow in the aqueduct utilizing our cine technique is abnormal. We have observed three circumstances in which there has been an absence of the

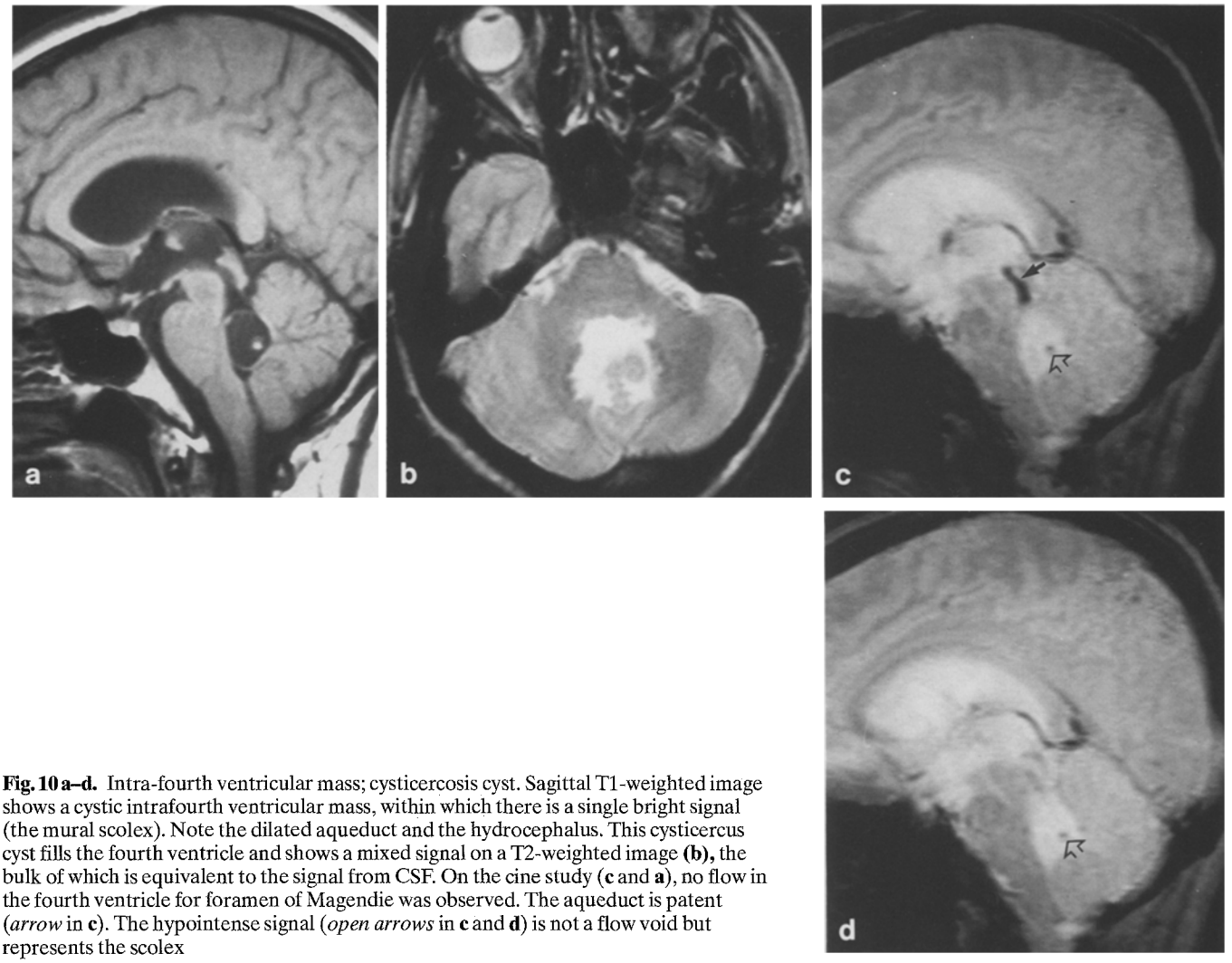

Fig. 10 a–d. Intra-fourth ventricular mass; cysticercosis cyst. Sagittal T1-weighted image shows a cystic intrafourth ventricular mass, within which there is a single bright signal (the mural scolex). Note the dilated aqueduct and the hydrocephalus. This cysticercus cyst fills the fourth ventricle and shows a mixed signal on a T2-weighted image **(b),** the bulk of which is equivalent to the signal from CSF. On the cine study (**c** and **a**), no flow in the fourth ventricle for foramen of Magendie was observed. The aqueduct is patent (*arrow* in **c**). The hypointense signal (*open arrows* in **c** and **d**) is not a flow void but represents the scolex

aqueductal flow void: (a) aqueductal stenosis/insufficiency (Fig. 7), (b) compression of the midbrain and aqueduct by a mass (Fig. 8), and (c) in third ventricular mass lesions which have resulted in a lack of propagation of the fluid wave through the third ventricle and into the aqueduct (Fig. 9). With aqueductal stenosis (Fig. 7), although the flow void in the aqueduct is absent, pulsatile flow from the inferior portion of the fourth ventricle into the cisterna magna may be observed, a fact which attests to the generation of an independent pulse wave at the fourth ventricular level. Mass lesions, whether infratentorial or supratentorial, can indirectly cause aqueductal obstruction by virtue of compression of the posterior third ventricle and/or the midbrain (Fig. 8). Obstruction of the CSF pathways above the aqueduct can diminish CSF flow, resulting in lack of fluid flow in the aqueduct. Such an example is shown in Fig. 9, where the obstructive nature of a third ventricular colloid cyst is seen.

Absence of flow in fourth ventricle and fourth ventricular outlet

Masses within or directly adjacent to the fourth ventricle or abnormalities located at the fourth ventricular outlet can alter the CSF dynamics by failing to allow normal propagation of a CSF pulse wave into the surrounding cisterns and cisterna magna (Figs. 10–12). Such a situation can result from a tumor, inflammatory process (Fig. 10), congenital abnormalities (Fig. 11), or adhesions in the fourth ventricle or in proximity to its outlet (Fig. 12). By a careful analysis of the flow patterns, one can determine if there is an obstruction to CSF flow and at what level the obstruction exists. We recognize that our imaging allowed an assessment of the fourth ventricular outlet only at the level of the foramen of Magendie. There were no attempts to visualize both foramina of Luschka. Appropriate observations can be crucial in certain cases where CSF diversionary procedures are being considered (Fig. 13). If CSF flow into an extracranial or extraspinal fluid collection exists, cine MR may be able to detect the opening from the SAS to the fluid collection, providing the flow is brisk enough to give a flow void (Fig. 12).

Alterations of intraspinal CSF flow

Hyperdynamic flow

Cystic abnormalities, whether inside or outside the cord, may show a flow void if there is pulsatile CSF within the cyst (Figs. 14, 15). Smaller intramedullary cystic lesions (less than two vertebral segments) may not show similar

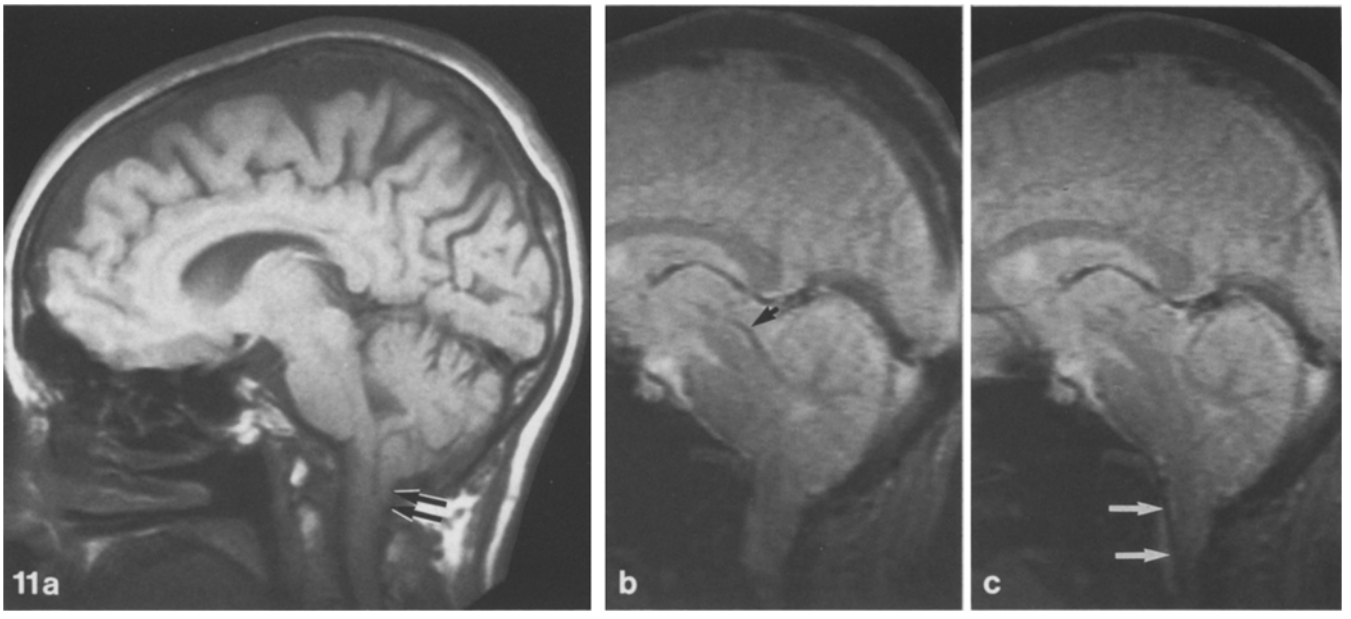

Fig. 11a–c. Chiari I malformation; lack of flow void in foramen of Magendie. Ectopic tonsils (*arrows* in **a**) situated well below the plane of the foramen magnum are noted in this sagittal T1WI **(a).** No ventriculomegaly is noted. Two frames from a cine MR study demonstrate aqueductal flow void (*black arrow* in **b**) and a flow void only in the ventral SAS at the cervicomedullary junction (*white arrows* in **c**). In both **b** and **c,** note the lack of flow from the fourth ventricle into the foramen of Magendie. The presumption is that normal flow from the fourth ventricle via the foramina of Luschka is present, so that there is no hydrocephalus

signal voids (Fig. 16), either because of the small size of the cyst or because of dense adhesions around the periphery of the residual cord which prevents expansion and contraction of the cord cyst. In fact, Post [17] demonstrated a posttraumatic spinal cord cyst which showed no pulsatile flow or turbulence on cine MR, but when the dura was opened at surgery and the adhesions lysed, sonography demonstrated a markedly turbulent intramedullary cyst.

Signal voids are commonly seen in congenital and large posttraumatic syrinx cavities [25], in benign cysts above intramedullary tumor (i.e. benign cystic dilatation of the central canal) [16], but not in cysts within neoplastic masses. We have observed long intramedullary cystic segments in patients examined months to years following severe cord trauma and these appear similar to what is illustrated in Fig. 15. Areas of myelomalacia (termed "microcystic myelomalacia") while appearing nearly equivalent to true cord cysts on T1 and T2WIs (long T1 and T2 relaxation times) are markedly different from true cysts on cine MR, in that they show no pulsatility or turbulence (Fig. 17). In the end however, it is intraoperative sonography [25] which most clearly distinguishes a true cyst from myelomalacia.

Despite the theory that congenital syringomyelic cavities are connected through the medulla via the obex to the fourth ventricle, we have not observed on cine MR a continuous flow void from the fourth ventricle to the syrinx. This may be related to the slice thickness (6 mm) in comparison with the usually narrow portion of the syrinx as it passes caudad at the level of the decussations of the pyramids.

Block of CSF flow

Normally (Figs. 3, 4) a CSF flow void can be identified throughout the cervical subarachnoid space (most prominent ventrally) as the pulse wave travels first in a caudal direction following cardiac systole. As illustrated previously, cranial flow of CSF during cardiac diastole can be observed well on the phase images (Fig. 4). Any lesion within the thecal sac or one which compresses the thecal sac can alter this normal caudad-craniad CSF flow. Close inspection of the closed loop cine MR can indicate whether the flow in the SAS is normal as in Figure 17 or whether there is a block of flow (Fig. 16). If a question still exists as to the presence of a block after evaluation of the routine magnitude reconstructed cine images, phase reconstructed images may be helpful, because these are, as described earlier, more sensitive to fluid motion.

Discussion

Although MR has the ability to detect moving material such as blood [26, 27] and CSF, the major attention of clinical investigators has been directed towards MR angiography [28] for evaluation of the vasculature of the head and neck. Little attention has been given to the evaluation of intracranial or intraspinal CSF flow. Those attempts which have been made involve the use of static images to determine whether or not there is CSF flow [7, 11]. We have, on the other hand, employed a closed loop cine method which allows the incorporation of a dynamic CSF sequence into a routine MR study whenever abnormalities of CSF flow are suspected.

When our observations concerning areas of CSF flow void in normal volunteers are compared to previous reports of the incidence of visualization of the aqueduct and

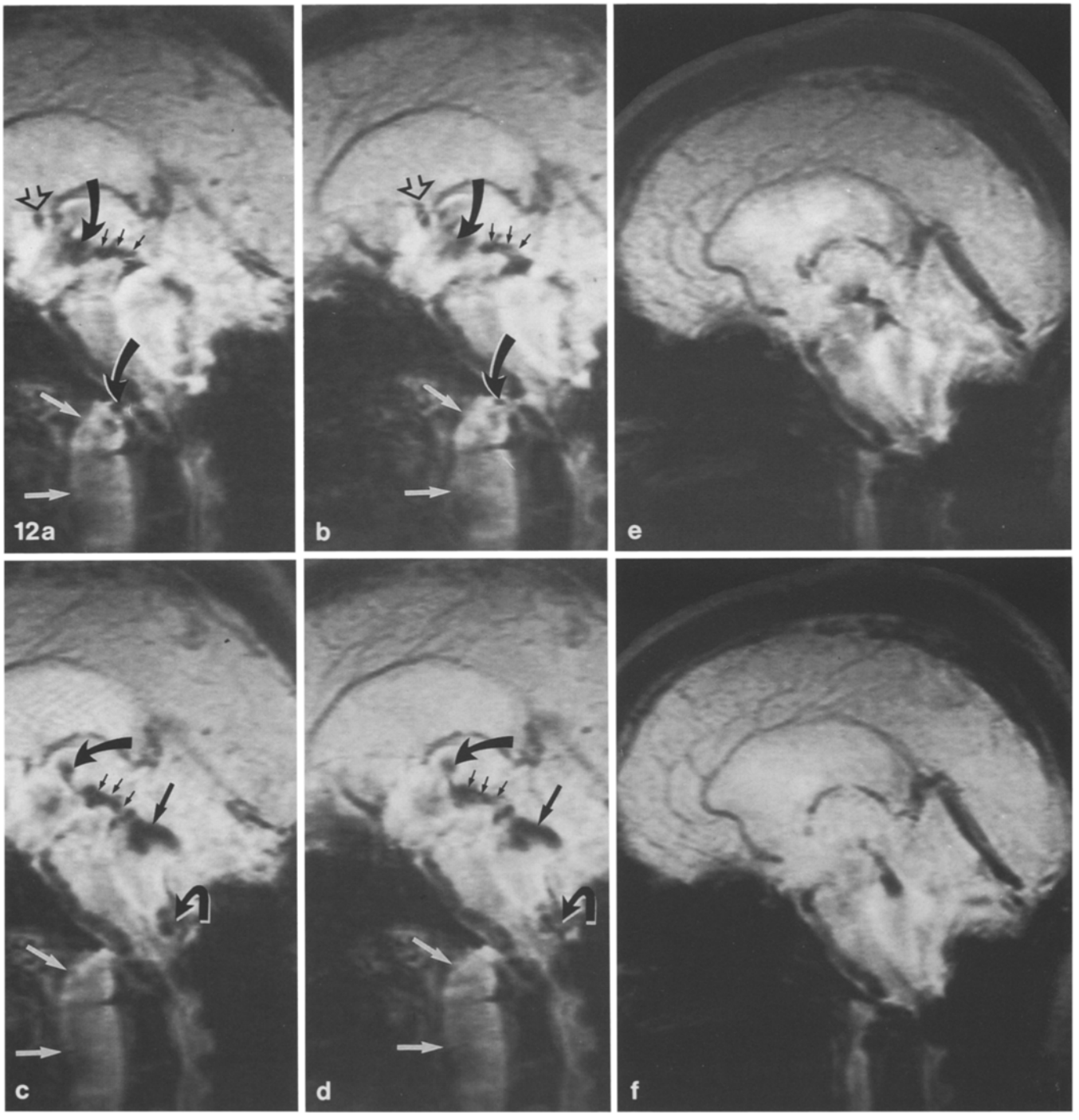

Fig. 12 a–f. Adhesions at base of skull and anterior spinal pseudomeningocele (pre and post shunting). In a patient with a fracture through the base of the skull and C1–C2 subluxation, wire stabilization posteriorly from the basiocciput to the upper cervical spine was performed (explaining the marked signal dropout at the skull base). Cine MR demonstrated an abnormal CSF flow pattern; specifically, 4 frames prior to ventricular shunting showed hyperdynamic flow (*straight single arrow* in **c** and **d**) within an enlarged fourth ventricle, a prominent to-and-fro pulse of CSF through a widened aqueduct (*short arrows* in **a–d**), significant hyperdynamic flow void in the posterior third ventricle *(curved arrows)* and reflux of the CSF through the foramen of Monro (*open arrowheads* in **a** and **b**) into the lateral ventricle. Anterior to the cervical spine from C1 to C2, a post-traumatic pseudomeningocoele is seen (*white arrows* in **a–d**). Flow void of CSF (*curved white arrows* in **a** and **b**) from the premedullary cistern into the pseudomeningocoele via a tear of the dura and arachnoid is identified. No flow out of the fourth ventricle into the cisterna magna could be observed but considerable turbulent flow at the foramen of Magendie was seen (*bent white arrows* in **c** and **d**). A lateral ventricular diversionary procedure (ventriculo-peritoneal shunt) was subsequently performed and the patient was imaged with cine MR thereafter (**e** and **f**). In these two frames, note the diminished flow void in the third, aqueduct and fourth ventricles compared to **a–d.** The prominent retrograde flow through the foramen of Monro is no longer observed. Decrease in size of the anterior pseudomeningo coele is noted and no longer was a flow void into this fluid collection identified

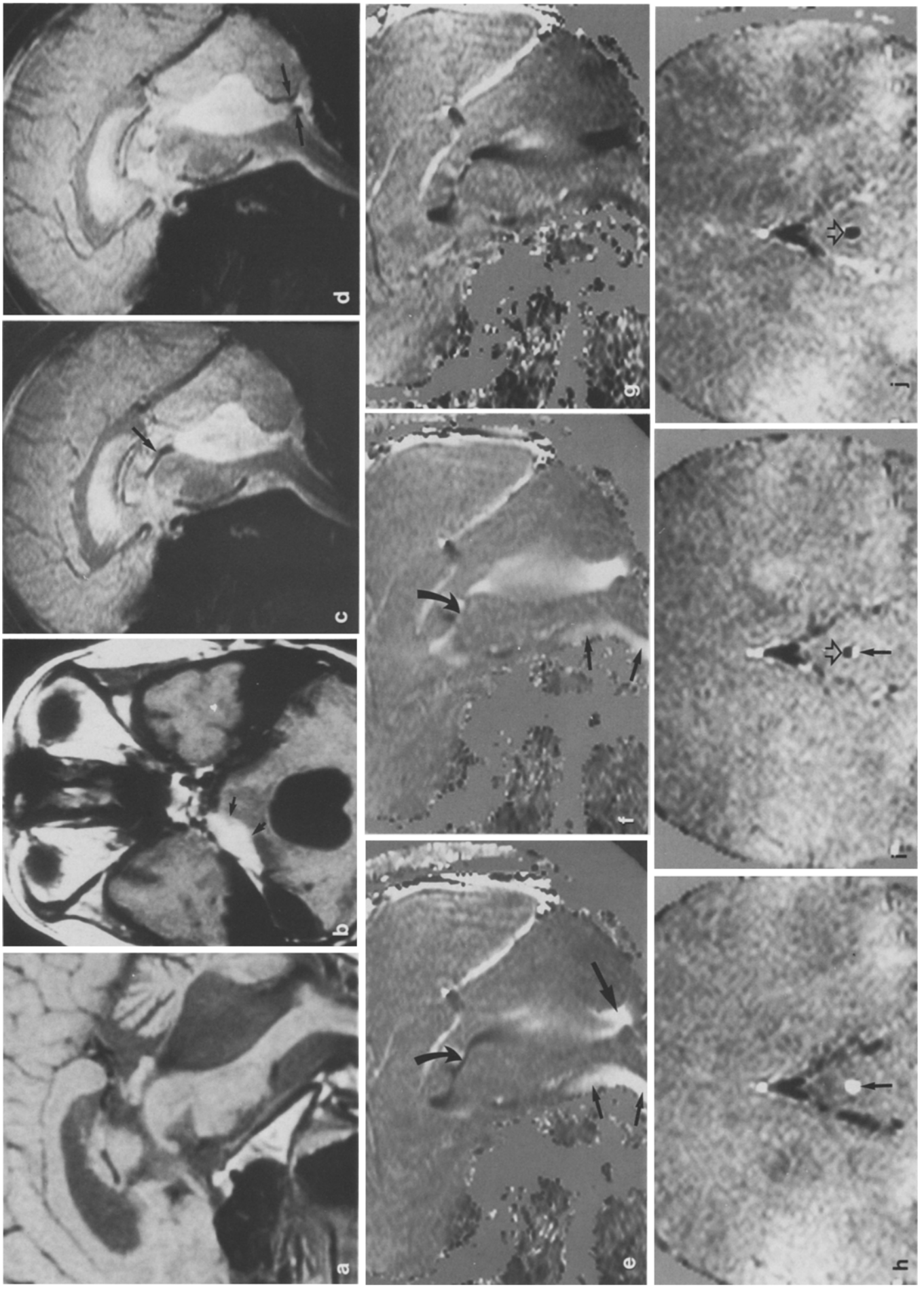
a
b
c
d
e
f
g
h
i
j

the foramen of Magendie, it appears that cine MR is more sensitive than static MR imaging in detecting fluid flow. Specifically, Sherman [29] reported varying incidence of flow voids in the aqueduct and foramen of Magendie depending on the degree of ventriculomegaly. When no ventriculomegaly was present an aqueduct flow void was noted in 67% and a foramen of Magendie flow void in 39%. These percentages increased with increasing ventriculomegaly. Our clinical material shows that with the cine MR technique as described above, these structures are routinely seen. It is emphasized however, that the degree of flow void in the foramen of Magendie normally varies from patient to patient, a fact which relates to its size and location relative to the mid-sagittal plane.

The clinical significance of this technique is apparent when one is either trying to assess whether surgical intervention may be efficacious or when one wishes to assess the patterns of flow during an MR examination to improve diagnostic accuracy. When confronted with a hydrocephalic patient in whom there is either no atrophy or mild atrophy, a frequent problem from an imaging standpoint is deciding whether there is insufficient flow through the aqueduct or whether there is a form of extraventricular communicating hydrocephalus (e.g. normal pressure hydrocephalus). As Fig. 1 demonstrates, a flow void through the aqueduct is expected in normal patients and when this flow void is absent (Fig. 7) and there is no mass lesion to explain this finding, the presumption is that an insufficient or stenotic aqueduct is present. Even when aqueductal compression is suspected because of a mass lesion, cine MR provides the confirmation that the ventriculomegaly is a consequence of aqueductal kinking or compression (Fig. 8). This can be of some importance when deciding whether ventriculomegaly is mainly a result of treatment (postoperative/postradiation/postchemotherapy) or whether the ventriculomegaly is partially or mainly on a mechanical basis. In the latter situation, a ventricular shunt may be indicated. The ability to visualize fluid flow within the posterior third ventricle and aqueduct depends, of course, on the propagation of the fluid wave through this portion of the CSF pathway. One would except therefore that a mass within the third ventricle would result in a diminished or absent aqueduct flow void sign (Fig. 9). It must be remembered therefore, that abnormalities other than of the aqueduct itself may cause such cine MR abnormalities.

Our experience with patients suspected of having normal pressure hydrocephalus (NPH) is limited. It was initially our hope that a hyperdynamic flow state in the aqueduct and fourth venricle could be used as a specific sign for NPH. To date, we have examined two patients with the classical clinical triad of NPH (gait apraxia, dementia, and urinary incontinence), one of whom had marked fluid turbulence similar to that shown in Figure 5. However, the other patient with NPH had a cine MR which was judged to be nearly normal (Fig. 6). To complicate this issue even further, we have observed a hyperdynamic CSF flow pattern in patients with cerebral atrophy and none of the clinical signs of NPH. Obviously, more patients with NPH need to be studied before any conclusions can be reached concerning the role of cine MR in evaluating this clinical problem, but our preliminary impression is that this issue is probably more complex than a qualitative evaluation of CSF dynamics alone can discern. With the calculation of actual CSF velocities using phase maps, a more specific pattern of NPH in terms of flow profiles, may be possible.

Since there is normally flow out of the fourth ventricle through the foramen of Magendie and into the cisterna magna (Figs. 1, 2), outlet obstructions resulting in hydrocephalus are well defined with cine MR. To date, we have evaluated only the foramen of Magendie and not the foramen of Lushka; however, evaluation of the latter should also be possible. Sagittal midline cine images as illustrated here are most rewarding because the CSF pathways can be followed as a continuum. Lesions adjacent to the fourth ventricle or within the fourth ventricle (Fig. 10) may cause outlet compression and result in an absent flow void; however, one must be certain that the plane of the scan encompasses the foramen of Magendie. Congenital abnormalities such as tonsillar ectopia (Fig. 11) can result in diminished or absent flow through the foramen of Magendie and in those cases where ventriculomegaly is not present, the presumption is that fluid had exited the fourth ventricle via the lateral foramina. In such cases more CSF flow ventrally at the cervicomedullary junction and within the ventral subarachnoid space in the upper cervical spine would be expected and has been noted (Fig. 11). Adhesions, whether secondary to trauma (Fig. 12), prior surgery, or inflammatory processes may also cause an abnormality of CSF flow. Cine MR can be helpful in determining the level of obstruction in cases of complex hydrocephalus, i.e. where any one of multiple adhesions or masses could ex-

Fig. 13a–j. Question of trapped fourth ventricle. Sagittal T1WI **(a)** and axial post-gadolinium **(b)** MR scans were performed in a patient with a previously subtotally resected right cerebellopontine angle meningioma (*arrows* in **b**). A functioning ventriculo-peritoneal shunt was in place and despite normal sized lateral ventricles, the fourth ventricle was markedly enlarged, raising the possibility of a trapped fourth ventricle (i.e. obstructed aqueduct and fourth ventricular outlets). Two cine MR frames (**c** and **d**) demonstrate both a patent aqueduct (*arrow* in **c**) and a patent foramen of Magendie (*arrows* in **d**). Phase imaging in the sagittal **(e–g)** and coronal **(h–j)** planes more clearly display the CSF flow dynamics. Caudal (hyperintense) flow of CSF out of the fourth ventricle (*straight black arrow* in **e**) preceeds caudal (hyperintense) flow throught the aqueduct (*curved arrow* in **f**). In fact, **e** shows that there is caudal flow of CSF in the foramen of Magendie is occurring while there is still cephalad flow (hypointense) within the aqueduct *(curved arrow)*. Expansion of the brain during systole forces caudal flow of CSF in the basal cisterns and anterior cervical SAS (*arrows* in **e** and **f**). During diastole **(g),** cephalad CSF flow (hypointense) is seen in the fourth ventricle, aqueduct, posterior third ventricle, anterior SAS and basal cisterns. Coronal cine MR **(h–j)** through the mid aqueduct showed caudal flow in the aqueduct (*arrow* in **h**), then an interval when some CSF was flowing cephalad (*open arrowhead* in **i**) and some CSF was flowing craniad (*straight arrow* in **i**), and then, cranial CSF flow (*open arrowhead* in **j**). Patency of CSF pathways was demonstrated on these studies, thus ruling out an isolated or trapped fourth ventricle. We postulated that the enlarged fourth ventricle was due to post-surgical changes

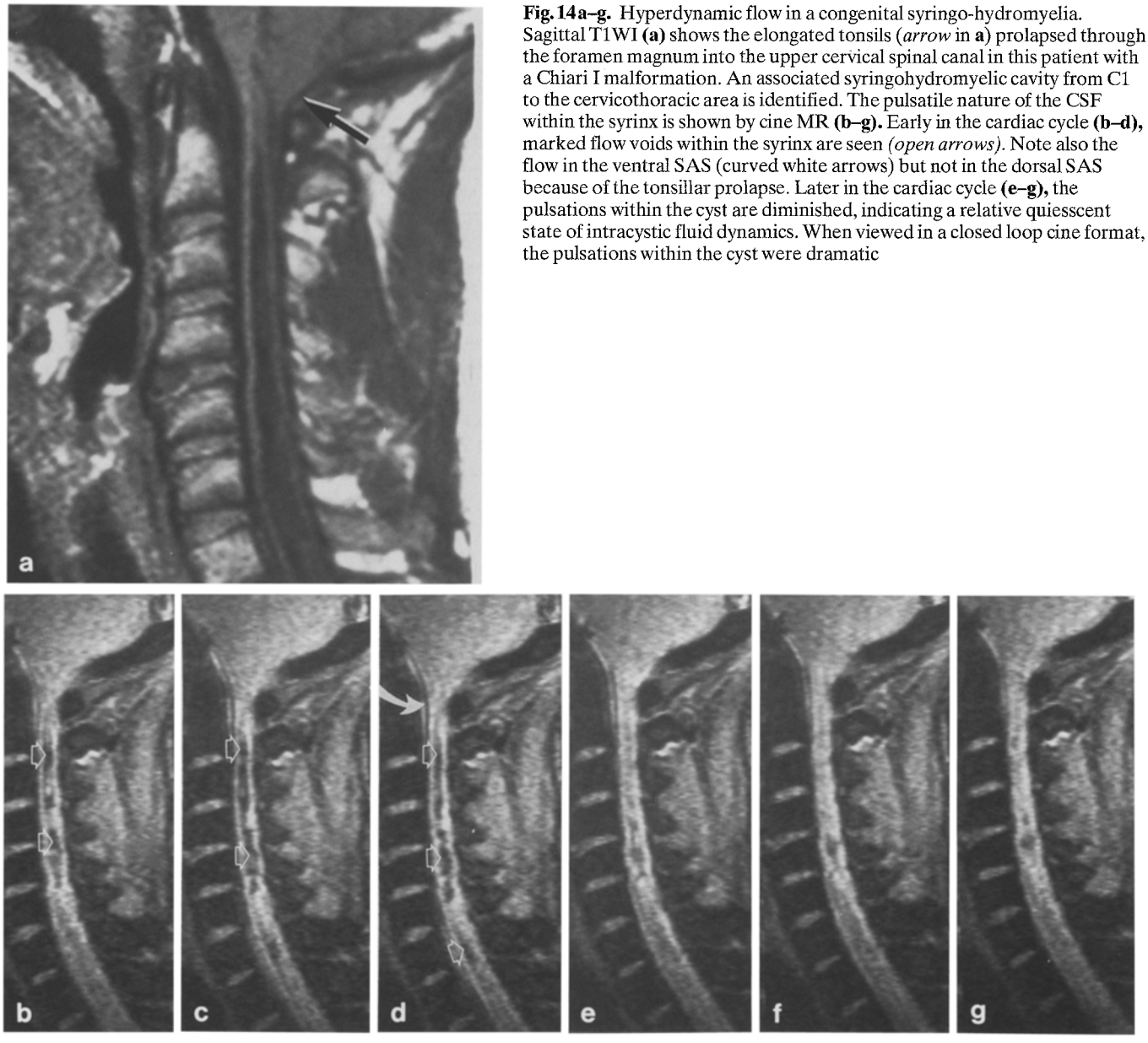

Fig. 14a–g. Hyperdynamic flow in a congenital syringo-hydromyelia. Sagittal T1WI **(a)** shows the elongated tonsils (*arrow* in **a**) prolapsed through the foramen magnum into the upper cervical spinal canal in this patient with a Chiari I malformation. An associated syringohydromyelic cavity from C1 to the cervicothoracic area is identified. The pulsatile nature of the CSF within the syrinx is shown by cine MR **(b–g).** Early in the cardiac cycle **(b–d),** marked flow voids within the syrinx are seen *(open arrows).* Note also the flow in the ventral SAS (curved white arrows) but not in the dorsal SAS because of the tonsillar prolapse. Later in the cardiac cycle **(e–g),** the pulsations within the cyst are diminished, indicating a relative quiesscent state of intracystic fluid dynamics. When viewed in a closed loop cine format, the pulsations within the cyst were dramatic

plain the ventriculomegaly. As Fig. 13 illustrates, demonstrating flow from the outlets of the fourth ventricle may be quite an important observation when consideration is being given to a possible fourth ventricular shunt in cases of a suspected trapped ventricle.

The use of phase imaging both in the head and spine (Figs. 2, 4, 13) will, in our opinion, assume an increasingly important role in the analysis of CSF flow states. The reason for this is the increased sensitivity of phase mapping to fluid flow. It is possible to have magnitude reconstructed images in which no flow is identified but where the phase reconstructions will show some CSF flow, albiet slow, through the area of clinical interest. We have recently incorporated phase imaging into our routine cine MR procedures in order to make the sequence as sensitive to flow as possible. This type of imaging and data acquisition allows the calculation of flow velocities which, in the future, may be employed in flow analysis.

CSF flow patterns in spinal abnormalities can have significant implications for diagnosis and treatment. In our experience, the most useful role for spinal cine MR is in the evaluation of cystic lesions of the spinal cord. Cystic cord lesions may be secondary to trauma, intra- or extramedullary tumors, inflammatory process, arachnoiditis, or may be congenital [25, 30–35]. Itabashi [36] evaluated CSF flow in nine syrinx cavities and felt that in some cavities there was cranial movement of CSF while at the same time there was caudal CSF flow in the adjacent subarachnoid space. Peak flow of CSF in the syrinx was reported to be less (15–50 mm/s) than in the SAS (40–60 mm/s). This asynchrony in pulse waves could relate to a pulsatile delay through the walls of the cyst.

Correlating the patient's symptoms with the character of posttraumatic spinal cord cysts and with congenital syringomyelia cysts as seen on cine MR is particularly im-

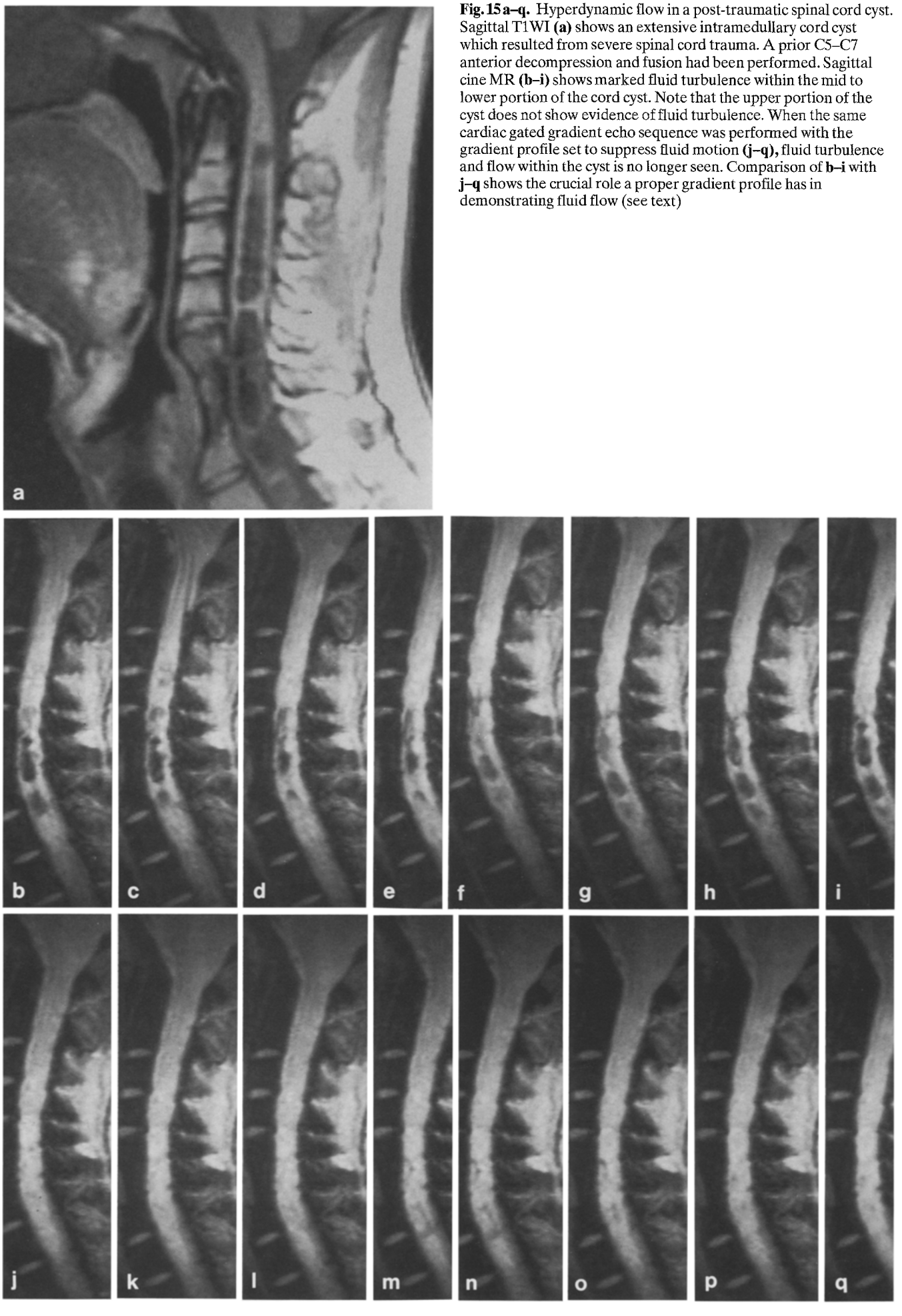

Fig. 15 a–q. Hyperdynamic flow in a post-traumatic spinal cord cyst. Sagittal T1WI **(a)** shows an extensive intramedullary cord cyst which resulted from severe spinal cord trauma. A prior C5–C7 anterior decompression and fusion had been performed. Sagittal cine MR **(b–i)** shows marked fluid turbulence within the mid to lower portion of the cord cyst. Note that the upper portion of the cyst does not show evidence of fluid turbulence. When the same cardiac gated gradient echo sequence was performed with the gradient profile set to suppress fluid motion **(j–q),** fluid turbulence and flow within the cyst is no longer seen. Comparison of **b–i** with **j–q** shows the crucial role a proper gradient profile has in demonstrating fluid flow (see text)

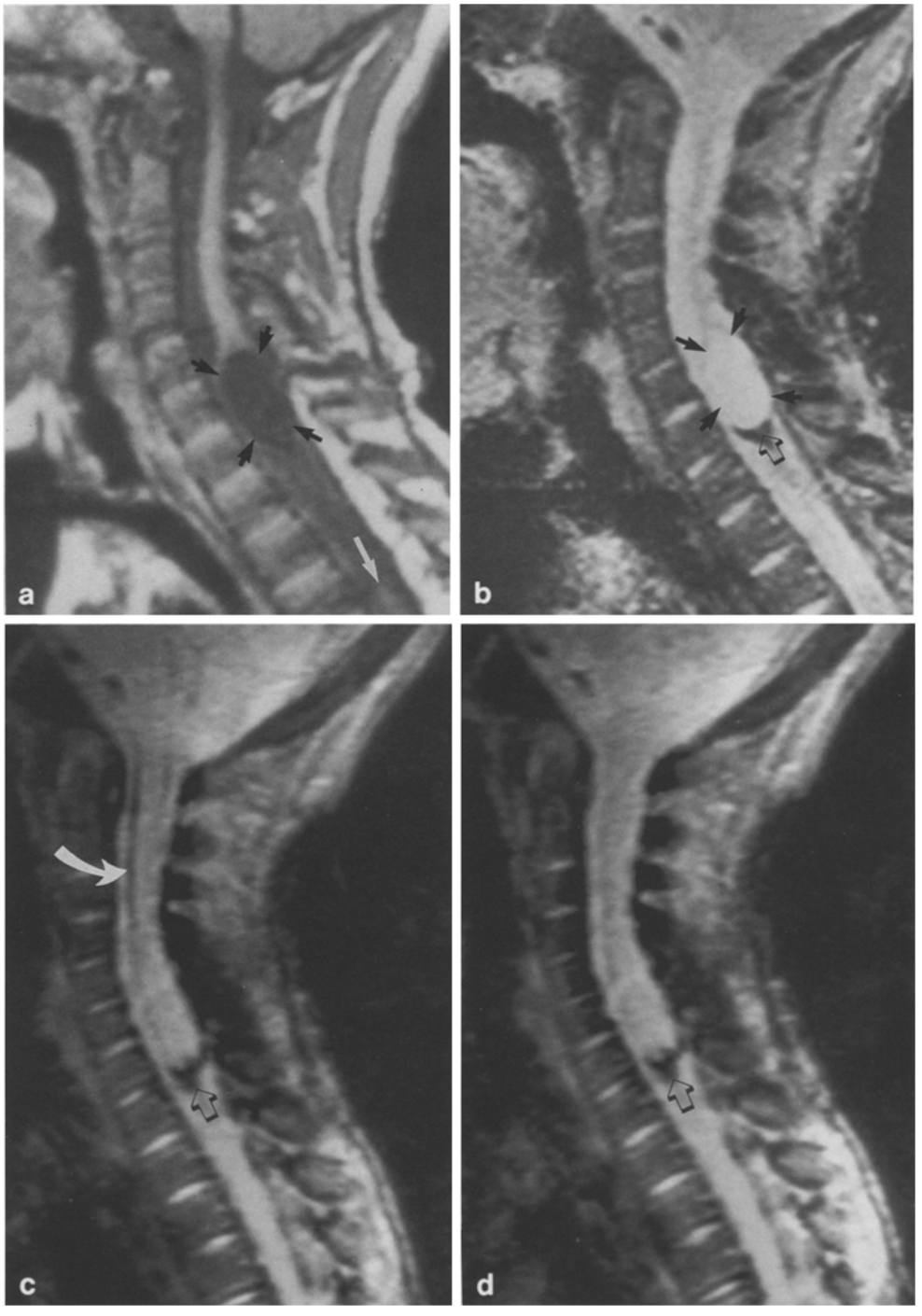

Fig. 16 a–d. Non-pulsatile post-traumatic spinal cord cyst and block of the subarachnoid space. A severe stretch injury to the spinal cord at the time of birth (breech delivery) resulted in quadriplegia. This MR, performed four years later because of new symptoms, shows focal cord enlargement associated with an area of well-defined signal hypointensity within the cord (*arrows* in **a**) at the C6–C7 level on the T1WI **(a)** and signal hyperintensity (*arrows* in **b**) on a sagittal gradient recalled echo image (383/13/10 degrees). A triangular area of marked hypointensity at the inferior end of the abnormality (*open arrowhead* in **b–d**) indicates the presence of an old hematoma. Below the cyst is **a** relative, but less marked hypointensity is present within the cord from T1–T3, indicating the presence of myelomalacia. The top of normal spinal cord tissue *(white arrow)* is identified from T4 inferiorly to the bottom of the field of view. Two frames of a cine MR (**c** and **d**) shows that there is no fluid pulsatility or detectable CSF flow within the area outlined by *arrows* in **a** and **b.** Note that the CSF pulse wave in the ventral and dorsal SAS (*curved arrow* in **c**) is not propagated past the C5 level, indicating a block to CSF flow by the large cyst and by intradural adhesions. We postulate that these dense intradural adhesions prevent the expansion/contraction of the cyst which accounts for the lack of pulsatile flow on cine MR (see text)

portant because such observations can have an impact on the decision of whether or not to operate. Specifically, a patient with new cord symptoms whose cine MR shows hyperdynamic CSF flow as in Fig. 14, might be a more likely candidate for a cyst to SAS shunting via catheter than a patient whose cyst does not have such an appearance. It is likely that CSF pulsations within the subarachnoid space are transmitted through the cyst walls and that turbulent flow of fluid within the cyst results unless, as mentioned earlier, dense adhesions around the cord prevent expansion and collapse of the cyst wall. This is the one situation where a cord cyst could be present but show no CSF pulsatility or turbulence. The observation on cine MR of fluid pulsatility within a cyst probably indicates that gradual cyst expansion is occurring with dissection of previously viable cord tissue and tracts. If surgery is not performed, patients with progressive neurological symptoms and this type of hyperdynamic fluid flow can be examined with time interval cine MR, not only to see if the cyst has enlarged (which can be accomplished with routine MR [37]), but also to see if the dynamics of the cord cyst have changed with time. Close examination of the fluid flow within these cysts shows a non-uniform, septated character of the cyst reflecting the well-known fibroglial scarring

Fig. 17a–e. Post-traumatic myelomalacic cord. Sagittal T1WI **(a)** shows ill-defined low signal intensity within an area of traumatized cord from C4 to C5 *(arrows)*. The cord is expanded at that level and compression of the ventral surface of the cord by bone is seen (*curved arrow* in **a**). Cine MR shows no fluid flow or turbulence within this area of the cord, but shows relative bright signal on these gradient echo images. Propagation of a synchronous fluid wave from above this level of injury to below it (*arrowheads* in **b**) indicates the lack of block in the SAS. The lack of flow void ventral and dorsal to the cord at the injury site is explained best by the presence of intradural adhesions

which traverses these cysts at irregular intervals causing variations in the flow patterns.

A question which frequently arises particularly in patients who have suffered prior cord trauma, is whether an area of low signal intensity within the cord represents a cyst or represents myelomalacia. Since myelomalacia can extend for some distance above and below the injury site because of demyelination, vascular insufficiency or metabolic changes, the length of the abnormality per se and its signal characteristics may not be sufficient to distinguish cyst from myelomalacia. In these instances, cine MR can be used since myelomalacia cord tissue will not show flow voids (Fig. 17), while larger cord cysts will (Fig. 15). It has been our experience that small, ovoid post-traumatic cysts usually do not demonstrate a flow void. A similar observation has been made by Sherman [37] using routine T2 weighted imaging. The clinical implications are clear – a cord cyst may be treated surgically, while myelomalacia is not. In addition, patients with a cyst measuring less than one vertebral segment in length are usually not surgical candidates.

The issue is less important in tumor cysts of the cord because these invariably show no fluid turbulence [37]. Such lesions are usually operated on whether by biopsy or

partial/complete resection, no matter what the cine MR shows. However, benign syrinx cavities above or below the spinal cord tumor, if large enough, can act like other cord cysts when evaluated by cine MR [16].

Blockage of the spinal CSF pathways similar to what is observed on myelography is possible with cine MR (Fig. 16). This diagnosis would be more simple in the cervical spine, where a prominent SAS flow void is normally observed. We believe that the use of cine MR provides a more direct and conclusive evidence of a CSF block in the spine than does the use of routine non-motion compensated T2 weighted images [38].

The relationship between CSF pulsations and the many variables which may affect them including systolic and diastolic blood pressure, pulse pressure, total intraspinal and intracranial CSF volume, intravascular blood volume, and respiration was not addressed in our present investigation. Du Boulay [2] addressed a few of these issues and noted a larger volumetric displacement of CSF at high and low arterial systolic pressures when compared to blood pressures in the mid-range. His explanation was that in higher arterial pressures, more arteriolar expansion in the brain occured, whereas in low blood pressure, there was a relative collapse of the veins and thus the loss of their ability to damp the brain pulsation: it was the pulse pressure (the systolic-diastolic difference) to which the amplitude of pulsation was proportional. It should be noted that for his particular study the patients were in a sitting position. Posture was also noted to have an effect upon respiratory variations of the CSF pulse. It is clear that further cine MR studies relating CSF dynamics to hemodynamics are warranted because such studies may indicate more variability in "normal" flow patterns than we now appreciate.

Conclusion

Cine MR, as described in this article, is capable of demonstrating both normal and abnormal intracranial and intraspinal CSF flow. Such a study can be easily added as an extra pulse sequence at the end of a routinely acquired MR exam. Magnitude reconstructed images can shown areas of decreased CSF flow and help explain the cause of hydrocephalus or in cases of spinal abnormalities, show obstruction to CSF flow. Analysis of cystic lesions of the cord or subarachnoid space can be furthered by cine MR and can help in distinguishing expanding cord cysts from myelomalacic changes. Phase mapping is more sensitive to fluid flow and may find increased utility in the future for both a subjective and an objective analysis of fluid flow. Surgical decisions can in part, be aided by careful analysis of these CSF cine MR studies.

References

1. DuBoulay GH (1966) Pulsatile movements in the CSF pathways. Br J Radiol 39: 255–262
2. DuBoulay GH, O'Connell J, Currie J, Bostic KT, Verity P (1972) Further investigations on pulsatile movements in the cerebrospinal fluid pathways. Acta Radiol 13: 496–523
3. Lane B, Kricheff II (1974) Cerebrospinal fluid pulsations at myelography: a videodensitometric study. Radiology 110: 579–587
4. Sherman JL, Citrin CM (1986) Magnetic resonance demonstration of normal CSF flow. AJNR 7: 3–6
5. Citrin CM, Sherman JL, Gangarosa RE, Scanlon D (1986) Physiology of the CSF flow-void sign: modification by cardiac gating. AJNR 7: 1021–1024
6. Sherman JL, Citrin CM, Gangarosa RE, Bowen BJ (1986) The MR appearance of CSF pulsations in the spinal canal. AJNR 7: 879–884
7. Sherman JL, Citrin CM, Bowen BJ, Gangarosa RE (1986) MR demonstration of altered cerebrospinal fluid flow by obstructive lesions. AJNR 7: 571–579
8. Bradley WG, Kortman KE, Burgoyne B (1986) Flowing cerebrospinal fluid in normal and hydrocephalic states: appearance on MR images. Radiology 159: 611–616
9. Bradley WG, Whittemore AR, Kortman KE, Caton WL, Garner JT (1989) Significance of the aqueductal cerebrospinal fluid flow void and deep white matter infarction on the outcome in patients with shunts for normal pressure hydrocephalus. Presented at the 75th Annual Meeting of the RSNA (Paper #312), November 27, 1989, Chicago IL
10. Rubin JB, Enzmann DR (1988) Differential flip-angle imaging of cerebrospinal fluid flow: clinical applications in the evaluation of syringomyelia. Presented at the 74th Annual Meeting of the RSNA (Paper#150), November 28, 1988, Chicago IL
11. Atlas SW, Mark AS, Fram EK (1988) Aqueductal stenosis: evaluation with gradient echo rapid MR imaging. Radiology 169: 449–453
12. Njemanze PC, Beck OJ (1989) MR gated intracranial CSF dynamics: evaluation of CSF pulsatile flow. AJNR 10: 77–80
13. Quencer RM, Hinks RS, Post MJD, Calabro G (1989) Intracranial flow of cerebrospinal fluid: qualitative and quantitative evaluation with CINE-MR imaging. Presented at the 75th Annual Meeting of the RSNA (Paper#313), November 27, 1989, Chicago IL
14. Post MJD, Quencer RM, Hinks RS (1989) Spinal CSF flow dynamics: It's qualitative and quantitative evaluation by CINE-MR. Presented at the 27th Annual Meeting of the ASNR (Paper #263), March 27, 1989, Orlando FL
15. Hinks RS, Post MJD, Quencer RM (1989) Quantitative evaluation of CSF flow dynamics in the spine. Presented at the 8th Annual Meeting of the SMRM, August 1989, Amsterdam, The Netherlands
16. Post MJD, Quencer RM, Green BA, Hinks SA, Sklar EM, Patchen S (1988) Cine-MR imaging in determining the flow characteristics of CSF and blood in spinal and intracranial lesions. Presented at the 74th annual meeting of the RSNA, Paper 579, November 30, 1988, Chicago, IL
17. Post MJD, Quencer RM, Green BA, Hinks SA, Horen M, Labus J (1988) The role of cine-MR in the evaluation of the pulsatile characteristics of post-traumatic spinal cord cysts. Presented at the 26th annual meeting of the ASNR, Paper #6, May 15, 1988, Chicago, IL
18. Quencer RM, Hinks RS, Pattany PH, Horen M, Post MJD (1988) Improved MR imaging of the brain using compensating gradients to suppress motion-induced artifacts. AJNR 9: 431–438
19. Elster AD (1988) Motion artifact suppression technique (MAST) for cranial MR imaging: superiority over cardiac gating for reducing phase-shift artifacts. AJNR 9: 671–674
20. Hinks RS, Quencer RM (1988) Motion artifacts in brain and spine MR. Radiol Clin North Am 26: 737–753
21. Thomsen C, Stahlberg F, Mogelvang J, Stubgaard M, Nordell B (1989) Fourier analysis of cerebrospinal fluid flow in cerebral aqueduct. Presented at the 75th Annual Meeting of the RSNA (Paper #311), November 27, 1989, Chicago IL
22. Enzmann DR, Rubin J, Pelc N (1989) Cine phase contrast maps of cervical cerebrospinal fluid motion. Presented at the 75th Annual Meeting of the RSNA (Paper #425), November 28, 1989, Chicago IL

23. Itabashi T, Arai S, Kitahura H, Watanabe T, Asahina K, Suzuki H (1988) Quantitative analysis of cervical cerebrospinal fluid pulsation. Presented at the 74th Annual Meeting of the RSNA (Paper# 569), November 30, 1988, Chicago IL
24. Levy M, DiChiro G, DeSouza B, McCullough DC, McVeigh E, Heffey D (1989) Fixed cord: effects of surgery and correlation with MR imaging. Presented at the 75th Annual Meeting of the RSNA (Paper # 428), November 28, 1989, Chicago IL
25. Quencer RM (1988) The injured spinal cord: evaluation with magnetic resonance and intraoperative sonography. Radiol Clin North Am 26: 1025–1045
26. Bradley WG (1988) Flow phenomena in MR imaging. AJR 150: 983–994
27. Nayler GL, Firmin DN, Longmore DB (1986) Blood flow imaging by cine magnetic resonance. J CAT 10: 715–722
28. Masaryk TJ, Modic MT, Ruggieri RM, Ross JS, et al. (1989) Three dimensional (volume) gradient echo imaging of the carotid bifurcation: preliminary clinical experience. Radiology 171: 801–806
29. Sherman JL, Citrin CM, Gangarosa RE, Bowen BJ (1986) The MR appearance of CSF flow in patients with ventriculomegaly. AJNR 7: 1025–1031
30. Castillo M, Quencer RM, Green BA, Montalvo BM (1987) Syringomyelia as a consequence of compressive extramedullary lesions: postoperative clinical and radiological manifestations. AJNR 8: 973–978
31. Quencer RM, El Gammal T, Cohen G (1986) Syringomyelia associated with intradural extramedullary masses of the spinal canal. AJNR 7: 143–148
32. Simmons JD, Norman D, Newton TH (1983) Preoperative demonstration of post-inflammatory syringomyelia. AJNR 4: 625–628
33. Pojunas K, Williams AL, Daniels DL, Haughton VM (1984) Syringomyelia and hydromyelia: magnetic resonance evaluation. Radiology 153: 679–683
34. Castillo M, Quencer RM, Post MJD (1988) MR of intramedullary spinal cysticercosis. AJNR 9: 393–395
35. Schlessinger AE, Naidich TP, Quencer RM (1986) Concurrent hydromyelia and diastematomyelia. AJNR 7: 473–477
36. Itabashi T, Arai S, Kithara H, Watanabe T, Asahina K, Suzuki H (1988) Quantitative analysis of syrinx fluid pulsation. Presented at the 74th Annual Meeting of the RSNA (Paper # 570), November 30, 1988, Chicago IL
37. Sherman JL, Barkovich AJ, Citrin CM (1986) The MR appearance of syringomyelia: new observations. AJNR 7: 985–995
38. Quent DJ, Patel SC, Sanders WP, Hearshen DO, Boulas RS (1989) Importance of absence of CSF pulsation artifacts in the MR detection of significant myelographic block at 1.5 T. AJNR 10: 1089–1095

R. M. Quencer, M.D.
University of Miami MRI Center
1115 N.W. 14th Street
Miami, FL 33101
USA